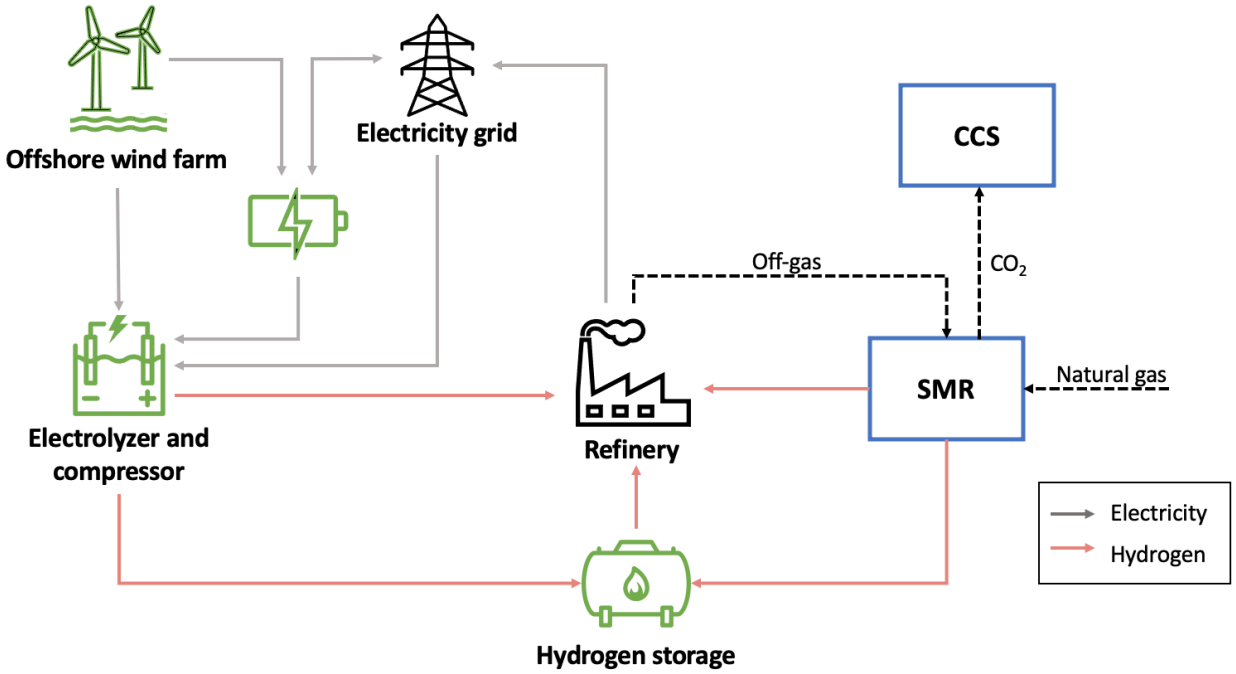

Hydrogen production for a net zero refinery

Cost-optimization of the interplay between a blue and green hydrogen production system

Master's thesis in Master Program Sustainable Energy Systems (MPSES)

ERIK AHLSTRÖM

OSCAR HULT

DEPARTMENT OF SPACE, EARTH AND ENVIRONMENT
CHALMERS UNIVERSITY OF TECHNOLOGY
Gothenburg, Sweden 2023
www.chalmers.se

Master's thesis 2023

Hydrogen production for a net zero refinery

Cost-optimization of the interplay between a blue and green hydrogen production system

ERIK AHLSTRÖM

OSCAR HULT

CHALMERS
UNIVERSITY OF TECHNOLOGY

DEPARTMENT OF SPACE, EARTH AND ENVIRONMENT
Division of Energy Technology
Energy Systems Modeling
Chalmers University of Technology
Gothenburg, Sweden 2023

Hydrogen production for a net zero refinery
Cost-optimization of the interplay between a blue and green hydrogen production system
ERIK AHLSTRÖM & OSCAR HULT

© ERIK AHLSTRÖM, 2023.
© OSCAR HULT, 2023.

Supervisor: Katarina Persson, Preem
Supervisor: Henrik Rådberg, Preem
Supervisor: Sofia Rosén, Department of Space, Earth and Environment
Supervisor: Alla Toktarova, Department of Space, Earth and Environment

Examiner: Lisa Göransson, Department of Space, Earth and Environment

Master's Thesis 2023
Department of Space, Earth and Environment
Division of Energy Technology
Energy Systems Modeling
Chalmers University of Technology
SE-412 96 Gothenburg
Telephone +46 31 772 1000

Cover: System boundary of the constructed optimization model.

Typeset in LaTeX
Printed by Chalmers Reproservice
Gothenburg, Sweden 2023

Hydrogen production for a net zero refinery
Cost-optimization of the interplay between a blue and green hydrogen production system
ERIK AHLSTRÖM & OSCAR HULT
Department of Space, Earth and Environment
Chalmers University of Technology

Abstract

In this thesis, a techno-economic cost-optimization model is applied to evaluate the interaction of a blue hydrogen system, which incorporates a steam methane reformer (SMR), carbon capture and storage (CCS), and a green hydrogen system. The green hydrogen system comprises an electrolyzer, hydrogen storage, battery storage, and an offshore wind farm with a power purchase agreement (PPA). The assessment focuses on achieving a net zero refinery in the year 2035. The model minimizes the total cost of investments and operation of CCS, and all technologies comprising the green system while meeting a continuous hydrogen demand. Sensitivity analysis is carried out to answer the two following questions; (i) What flexibility measures can reduce hydrogen production costs; and (ii) how do sensitive parameters affect the system composition and sizing of components? The results reveal that flexibility measures can be found in the electrolyzer, energy storage, and partly the SMR to manage wind variability. Furthermore, the model and its system composition are sensitive to the operational cost of the SMR. The resulting green hydrogen system consists of a 263 MW_{H2} electrolyzer, 469 MW offshore wind farm, 14 GWh hydrogen storage, and 2.3 MWh battery energy storage. It does together with a 297 MW SMR, employed with a 90 % capture rate CCS, meet a continuous hydrogen demand of 377 MW.

Higlights

- A resilient continuous hydrogen production system can be constituted of a blue and green hydrogen system.
- The green hydrogen is resilient to PPA prices but sensitive to OPEX of SMR.
- Employment of hydrogen storage is crucial for mitigating total system cost.
- Variability of different years has a small impact on the model's system composition.

Keywords: green hydrogen, flexibility, variability, power-purchase-agreement, net zero refinery.

Acknowledgements

Thanks to Henrik Rådberg, who gave us the opportunity to do our master's thesis at Preem. Your input has been quick and your involvement has been enthusiastic since the start of the thesis. Thanks to Katarina Persson, for your guidance in refinery processes. Thanks to our examiner Lisa Göransson, who is a well-known energy system modeler and yet has time for supervision meetings and long discussions regarding our work. Thanks to Alla Toktarova, who has been relentless with input and feedback even through her own commitment to finishing her own doctorial thesis. Finally, a special thanks to Sofia Rosén who has been there, no matter the time or question from day one.

Erik Ahlström & Oscar Hult, Gothenburg, May 2023

List of Acronyms

Below is the list of acronyms that have been used throughout this thesis listed in alphabetical order:

BECCS	Bio-Energy with Carbon Capture and Storage
CAPEX	Capital Expenses
CCS	Carbon Capture and Storage
EU ETS	European Union Emission Trading System
LCOE	Levelized Cost Of Electricity
LCOH	Levelized Cost Of Hydrogen
LNG	Liquefied Natural Gas
LP	Linear Programming
LIB	Lithium Ion Battery
LRC	Lined Rock Cavern
PAP	Pay As Produced
PPA	Power Purchase Agreement
OPEX	Operational Expenses
SMR	Steam Methane Reformer
SOC	State Of Charge
WF	Wind Farm

Contents

List of Acronyms **ix**

List of Figures **xiii**

List of Tables **xv**

1 Introduction **1**
1.1 Thesis Aim . . . 2

2 Theory **5**
2.1 Hydrogen system at traditional refineries . . . 5
2.1.1 Flexible hydrogen production at refinery . . . 6
2.2 Energy storage . . . 7
2.2.1 Hydrogen Storage . . . 7
2.2.2 Li-ion Batteries . . . 8
2.3 Power Purchase Agreements . . . 9
2.4 Carbon Capture and Storage (CCS) . . . 10
2.5 EU Emissions Trading System (EU ETS) . . . 11

3 Methods **13**
3.1 The linear optimization model . . . 13
3.1.1 Objective function . . . 15
3.1.2 Model constraints . . . 16
3.2 Economic calculations for technologies . . . 17
3.2.1 Operational cost of SMR . . . 18
3.2.2 Levelized Cost of Hydrogen . . . 18
3.2.3 Levelized cost of offshore wind power . . . 18
3.3 Compression of hydrogen . . . 19
3.4 Sizing of hydrogen storage . . . 19
3.5 Sensitivity Analysis . . . 19
3.5.1 The cost of offshore wind power . . . 20
3.5.2 The investment cost of hydrogen storage . . . 20
3.5.3 Transmission capacity and forecasted spot prices . . . 20
3.5.4 Operational cost of the SMR . . . 21
3.5.5 Wind profiles . . . 21

4 Results **23**
4.1 Reference case . . . 23
4.2 Sensitivity Analysis . . . 27
4.2.1 The cost of offshore wind power . . . 27
4.2.2 The investment cost of hydrogen storage . . . 31
4.2.3 Transmission capacity and forecasted spot prices . . . 34
4.2.4 Operational cost of the SMR . . . 38
4.2.5 Wind profiles . . . 43

5 Discussion **47**

6 Conclusion **49**

A Figures for technologies **I**

B Values of necessary parameters **III**

C Sensitivity analysis: Transmission capacity and forecasted spot prices **V**

List of Figures

1.1 Change in global hydrogen demand in million metric tonnes for the years 1975-2018. Data retrieved from IEA [2]. 2

2.1 Principle illustration of hydrogen consumption and production at traditional refinery. 6
2.2 A conceptual illustration of the three layers that seal the stored hydrogen gas - rock bed, concrete, and steel lining 8
2.3 Spot prices and mean PPA price for onshore wind power in SE3 (2020). 10

3.1 Schematic overview of the system investigated in this thesis. Technologies included in the green hydrogen system are shown in green, and technologies included in the blue hydrogen system are shown in blue. 14
3.2 The share of installed capacity of electricity generating technologies for Sweden 2019, Sweden 2050, and the total system 2050. 21

4.1 Distribution of costs for the hydrogen system. Note that *PPA*, *import* and *operational cost of the SMR* are related to the operational expenses of the hydrogen system. The capital expenses are annualized according to Equation (3.21). 24
4.2 Hydrogen supply from the electrolyzer, SMR and hydrogen storage, and the hydrogen demand for 1500 arbitrary hours (a). The wind power production from the offshore wind farm and the electricity consumption of the electrolyzer (b). 25
4.3 State of charge for the hydrogen storage during the time set of 8760 hours. The storage capacity is dimensioned by the time period between hours 4,500 and 5,300, where the state of charge goes from full to empty. 26
4.4 Battery charge and discharge (a), electricity import and export (b), electrolyzer electricity consumption and wind power production (c). 27
4.5 Total system cost in relation to the reference case (a), and levelized cost of hydrogen for different costs of offshore wind power (b). 28
4.6 Electrolyzer and wind farm capacities for different costs of offshore wind power (a). Hydrogen storage and battery storage capacities for different costs of offshore wind power (b). Note that energy storage capacities are given in different magnitudes. Hydrogen storage capacity is given in GWh and battery storage capacity is given in MWh. The reference cost of offshore wind power (PPA) is 53 EUR/MWh. 29
4.7 The annual hydrogen production from the hydrogen production technologies (SMR and electrolyzer) (a). Capacity factors for each hydrogen production technology (b). 30
4.8 Electricity trading with different PPA costs. Included in the trading is electricity import and export, and the curtailment that is a result of excess electricity from the offshore wind farm that cannot be utilized or exported due to model constraints. . 31
4.9 The relative change of total system cost (a), and LCOH for the green and blue hydrogen system (b). 32
4.10 Resulting electrolyzer and wind farm capacity a). Resulting in energy storage capacity for different specific investment costs of hydrogen storage. Hydrogen storage capacity is given by the right y-axis measured in GWh and battery capacity is given by the right y-axis measured in MWh in a logarithmic scale b) 33

4.11 The annual hydrogen production from the hydrogen production technologies (SMR and electrolyzer)(a), and capacity factors for each hydrogen production technology (b). 34
4.12 Electrolyzer and wind farm capacity for varying transmission capacities (a). Energy storage capacities with different available transmission capacities (b). Hydrogen storage capacity is given in GWh and battery storage capacity in MWh. 35
4.13 Wind profile and spot price correlation for spot prices from 2019 and forecasted spot prices for 2050. The wind profile is sorted and plotted by weekly average, and the spot prices are plotted with the same indexation as the sorted wind profile. The forecasted spot prices for 2050 are generated using input data from 2019. Note that the spot price peaks for 2050 are not seen in the figure (week 12 and weeks 31-32). 36
4.14 Electricity import, export, and curtailment for transmission capacities in the range 0-60 MW, with spot prices from 2019 and 2050 forecasted spot prices (a). Capacity factors for SMR and electrolyzer with transmission capacities in the range of 0-60 MW, with spot prices from 2019 and 2050 forecasted spot prices (b). Note that the y-axis does not start at 0. 37
4.15 Total system cost relative to the reference case (110 EUR/MWh$_{H2}$) for operational costs in the range 55-165 EUR/MWh$_{H2}$ (a). Levelized cost of hydrogen for operational costs in the same range (b). 38
4.16 Capacities for (a) electrolyzer and wind farm and (b) energy storages. 39
4.17 Hydrogen supply (a) and state of charge (b) for 2,000 hours when the dimensioning time period occurs. OPEX set to 55 EUR/MWh$_{H2}$. 40
4.18 Hydrogen supply with different operational costs for the SMR. In (a) and (b), the operational cost is set to 110 EUR/MWh and 137 EUR/MWh, respectively. The load of the SMR increases when the storage is discharged. With an operating cost of 165 EUR/MWh, seen in (c), the SMR is mainly operated on minimum load and does not increase in load during hydrogen storage discharge. 41
4.19 Export and import are suppressed with increased OPEX of the SMR, meanwhile curtailment increases. 42
4.20 Hydrogen production (a) and capacity factors (b) for the SMR and electrolyzer with operational costs of the SMR in the range 55-165 EUR/MWh. 43
4.21 Normalized wind profile and monthly, and yearly wind profile average for 2015. . . 44
4.22 Normalized wind profile and monthly, and yearly wind profile average for 2018. . . 45
4.23 Five cycles, one for each year, are measured over the simulated period. 46

C.1 Levelized cost of hydrogen for (a) 2019 and (b) 2050. VI
C.2 The relative change in total system cost for 2019 and 2050. VI

List of Tables

2.1 Costs for energy storage technologies. 9

3.1 Notations describing the model. 15

4.1 Numerical results for the reference case. 23
4.2 Capacity factor and resulting hydrogen storage, electrolyzer, and wind farm capacity. GIS 2019 is the reference case. 43
4.3 Resulting energy storage, electrolyzer, and wind farm capacities. 45
4.4 Import, export, and curtailment during each year in the consecutive model run. . . 46

A.1 Financial figures, technical lifetimes and efficiencies for respective technology used in the reference case. Figures for the CCS are I

B.1 Figures for the model's parameters used in the reference case. III

1
Introduction

In the European Green Deal, the European Union (EU) presents the transition plan for reaching zero greenhouse gas emissions by 2050 [1]. Green hydrogen production is one of the cornerstones in the transition plan to achieve the climate targets. There are two aspects to hydrogen that the Green Deal covers. The first aspect is that hydrogen is expected to play a key role in future energy systems as an energy carrier both for industry and transport. Electricity can replace fossil fuels for several uses, but some uses are more difficult to electrify than others. Within the transportation sector, road freight, shipping, and aviation are more difficult to electrify than passenger vehicles. Hydrogen can act as a substitute for these uses, either directly or by using hydrogen as feedstock when producing electrofuels. In industrial activities, such as steel or cement production, hydrogen can substitute fossil fuels as an energy carrier or a reactant in chemical processes. The European Parliamentary Research Service (EPRS) has also presented studies showing that an integrated energy system, where electricity is used to produce hydrogen and existing gas infrastructure is utilized, would be more cost-efficient rather than aiming for total electrification, resulting in costly grid extensions and energy storage solutions.

The second aspect of the Green Deal regarding hydrogen is the production of hydrogen. With 2018's levels, hydrogen production alone was responsible for carbon dioxide emissions of approximately 830 million tonnes globally. Hydrogen can be produced using different types of technologies and feedstocks, and depending on the production process and the resulting greenhouse gas emissions, hydrogen is classified using colors [2]. Steam methane reforming of natural gas is the primary method of hydrogen production, contributing to three-quarters of the global annual supply. The steam methane reforming process of natural gas has an average cost of 45 EUR/MWh and is associated with carbon emissions. The steam methane reforming process is classified as *grey hydrogen*. However, the steam methane reforming process can be combined with carbon capture and storage (CCS) to account for the carbon emissions related to hydrogen production. This way of producing hydrogen is classified as *blue hydrogen* and has an average cost of 60 EUR/MWh. An alternative to steam methane reforming is what is known as *green hydrogen*, where hydrogen is produced by electrolysis of water with renewable electricity, resulting in no greenhouse gas emissions. Depending on different assumptions and electricity prices, the average cost of green hydrogen is in the range of 75-167 EUR/MWh [1], assuming constant operation of the electrolyzer [2]. The Green Deal promotes blue and green hydrogen production to reduce the associated greenhouse gas emissions as the global hydrogen demand is expected to increase. International Energy Agency (IEA) [3] states that the global hydrogen demand has threefold since 1975 when the global demand for hydrogen was 18.2 million metric tonnes to 2018 levels of 73.9 million metric tonnes. In Figure 1.1, the global demand for hydrogen over the period 1975-2018 is presented [3]. After the pandemic in 2021, global hydrogen demand reached a new all-time high, measuring 94 million metric tonnes. This did correspond to 2.5 % of the global energy consumption [4].

[1] Conversion ratio: 0.033 MWh/kg H_2

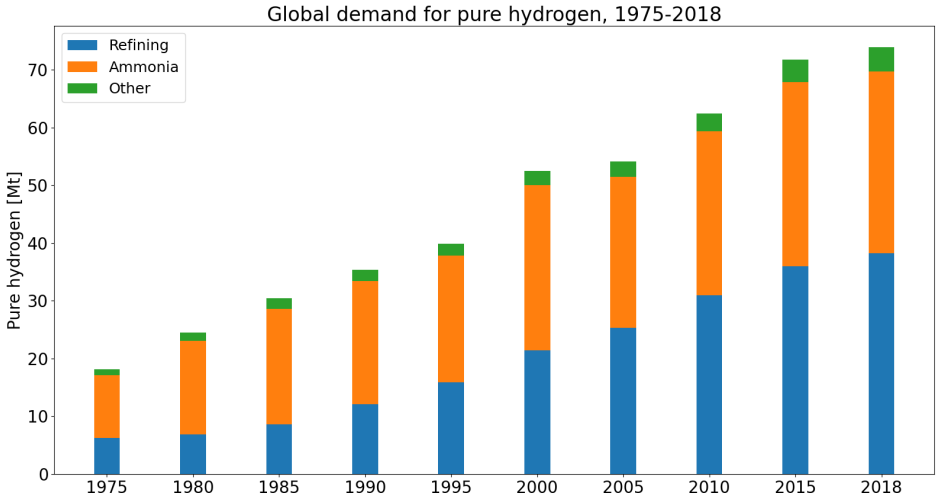

Figure 1.1: Change in global hydrogen demand in million metric tonnes for the years 1975-2018. Data retrieved from IEA [2].

The largest fuel manufacturer in Sweden, Preem, has two refineries that are located on the west coast of Sweden, in Lysekil and Gothenburg [5]. The refineries are among the most environmentally efficient refineries in the world [6]. Preem aims to become climate neutral by the year 2035, which implies climate-neutral operations with net-zero emissions throughout the value chain of fuel production. Preem has implemented a number of strategies linked to the ambitious climate targets. The first strategy is to adapt their refineries so that fossil crude oil can be replaced by biogenic feedstock, such as waste materials from forestry, agriculture, and the food industry. The second strategy is to integrate carbon capture and storage (CCS) facilities at their refineries to mitigate CO_2 emissions. When CCS is combined with biogenic feedstock negative emissions can be obtained by the concept Bio Energy Carbon Capture and Storage (BECCS). In addition to CCS, Preem also investigates the possibility to utilize captured carbon dioxide in their processes. This concept is known as Carbon Capture and Utilization (CCU). The third strategy regards replacing natural gas with biogas, and fossil-free hydrogen production. Natural gas is mainly used for hydrogen production at refineries and is also one of the main contributors to carbon emissions at the refineries. The fourth strategy is to adapt and include product offerings in line with the demand of a sustainable society. Electrification of road transports and energy efficiency measures reduce the need for liquid fuels. The new product offerings include hydrogenated vegetable oil (HVO), renewable aviation fuel, and electrofuels.

1.1 Thesis Aim

The thesis aims to investigate the interplay between a green hydrogen system and an existing steam methane reformer (SMR) with employed CCS, to find a cost-optimal strategy to meet the continuous hydrogen demand at the net zero refinery. The green hydrogen system includes an offshore wind farm, electrolyzer, batteries, and storage. The investigated refinery is Preemraff in Lysekil. The temporal scope of this study is the year 2035, when Preem aims to become climate neutral throughout the value chain of fuel production. To achieve the aim of this thesis, a series of specific objectives are defined:

- Develop a cost-optimization model to analyze the interplay between a refinery's blue and green hydrogen systems.
- Identify flexibility measures in the hydrogen system to reduce the production cost of hydrogen.
- Identify sensitive parameters and analyze the robustness of the system, regarding operation

strategy and system dimensions.

2
Theory

The theory section covers current hydrogen production at existing refineries (2.1), different sorts of energy storages (2.2), how power purchase agreements can be designed (2.3), carbon capture and storage (2.4), and finally how the European Union's Emission Trading System is designed (2.5).

2.1 Hydrogen system at traditional refineries

In today's refineries hydrogen play several key roles. Hydrogen is both a reactant in chemical reactions and a byproduct from certain processes, see Figure 2.1. The main purpose of hydrogen at refineries is for *hydrotreating*, which is a catalytic process where unsaturated hydrocarbons are converted to paraffin by adding hydrogen [7]. In the process, sulfur is removed from the hydrocarbon. Hydrogen is also used for *hydrocracking* where heavier oil fractions are upgraded to lighter fractions with higher market value [8].

There are two commercial forms of hydrogen production at traditional refineries: *steam methane reforming* (SMR) and utilizing *byproduct hydrogen* from processes [9]. In the SMR a light hydrocarbon and steam are catalytically cracked at high temperatures. The most common feedstock for the SMR is natural gas, where methane is the main component. Modern refineries are usually designed with the possibility to use other available sources of hydrocarbons as feedstock in the SMR [10]. Such available sources of hydrocarbons are often off-gases from other processes at the refinery, containing a mixture of different light hydrocarbons and hydrogen. The output from the SMR is synthesis gas, which consists of hydrogen, carbon dioxide, and carbon monoxide. The carbon monoxide is further reacted into carbon dioxide, and the carbon dioxide and hydrogen are separated [11]. Hydrogen is also produced as a byproduct from the *catalytic reforming unit* (CRU), where naphtha is reformed into high-octane products. Depending on the quantity of octane products that is produced in the refinery the amount of byproduct hydrogen varies. Other minor byproduct sources of hydrogen are the gasification of petroleum residues and coke and recovery from the refinery off-gases. Byproduct and recovery streams of hydrogen are complemented with the bulk production of hydrogen that is produced in the SMR [12].

The catalytic process in the SMR is endothermic, which means that heat is required [13]. The catalytic reaction requires high-temperature steam of around 700-1000°C and 3-23 bar to separate the hydrogen from the feedstock. The high temperatures of the SMR limit how the unit can be operated. Fast load shifting can therefore result in internal thermal stresses and reduce the expected lifetime of the unit. Except for technical limitations, other factors at the refinery limit the operation of the SMR. Refineries that are designed to utilize off-gases as feedstock in the SMR are constrained by the availability of off-gases at the refinery. Without storage for off-gases, the minimum load of the SMR is determined by the excess off-gases available at the refinery.

Both the refining industry and the transportation sector are facing challenges to reduce the climate impact of fuel production and fuel usage. The challenges are associated with finding substitutes for fossil fuels, and the demand for biogenic fuels is therefore expected to increase in the near future [14]. The electrification of internal combustion passenger vehicles is an ongoing process, but other parts of the transportation sector are more difficult to electrify, such as aviation, shipping, and long-distance trucks. The demand for biofuels and electrofuels is therefore expected to increase in

the future [15] [16]. For refineries, this means a shift away from refining petroleum to processing biogenic feedstock and waste materials. By shifting to biogenic feedstock the refining process will be affected in certain ways. First of all, the biogenic feedstock at the refinery means that there will be biogenic off-gases available at the refinery. These off-gases can generate net negative emissions if CCS is employed (BECCS). Secondly, Preem is not planning to operate the CRU for hydrogen production in a climate-neutral refinery configuration, due to low volumes of CRU feedstock when operating their refineries on biogenic feedstock. Additionally, the biogenic feedstock refining process requires more hydrogen than refining petroleum products. Biogenic feedstock contains oxygen and double bonds, which requires more hydrogen to saturate the hydrocarbons. Hydrogen is also used as feedstock in the process of producing electrofuels. However, the demand for electrofuels in the near future (until 2035) is uncertain and is therefore excluded from this thesis work. The hydrogen supply from the catalytic reformer unit is also neglected, and the assumed hydrogen demand is in line with one of the scenarios of Preem's expected annual demand in the year 2035 of 100,000 tonnes (3300 GWh) in Lysekil. Further, the hydrogen demand at the refinery is assumed to be continuous and constant over the year.

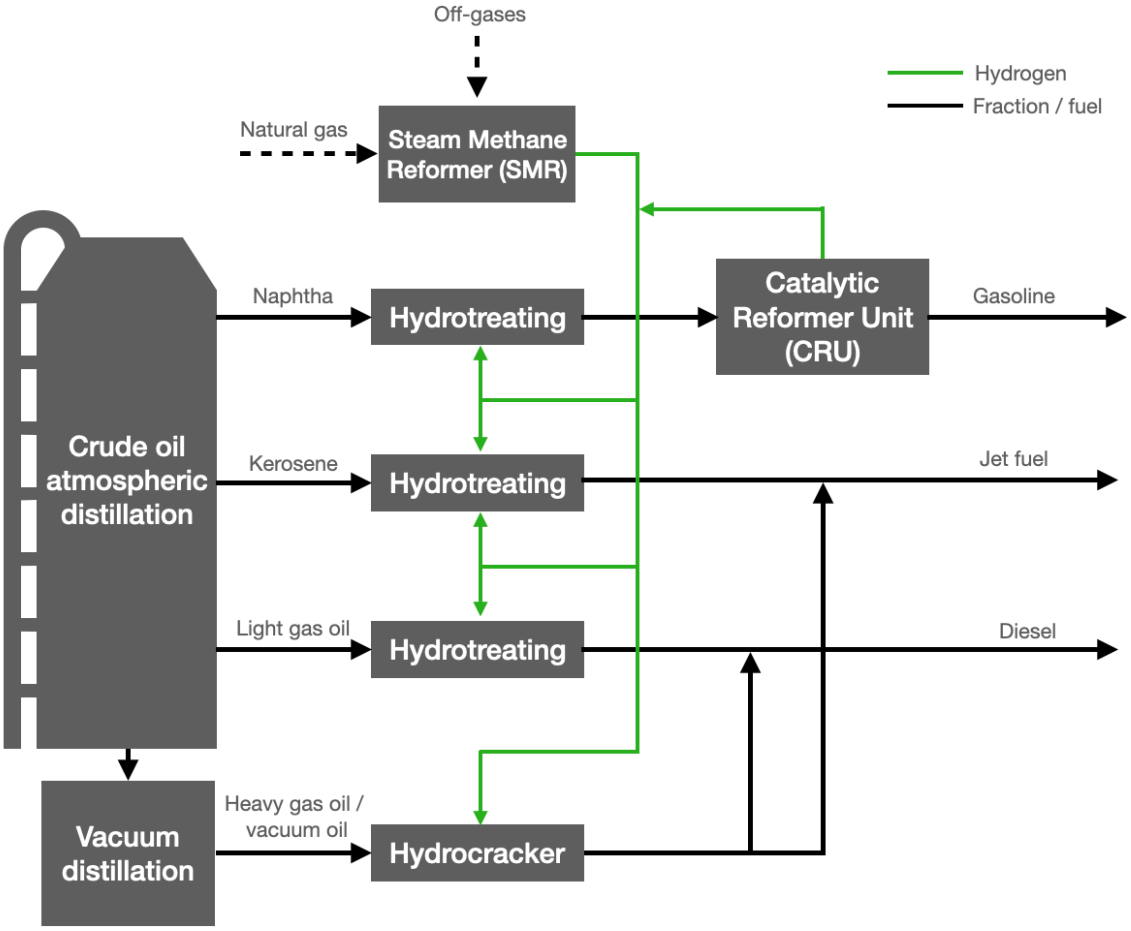

Figure 2.1: Principle illustration of hydrogen consumption and production at traditional refinery.

2.1.1 Flexible hydrogen production at refinery

An alternative to producing hydrogen by steam methane reforming is through water electrolysis, where an electric current splits water into hydrogen and oxygen. Compared to steam methane reforming, the electrolysis process comes with no carbon emissions, if the electricity is carbon neutral. The electrification of hydrogen production at refineries will increase the demand for electricity and the electrical load on the electricity system. From a system perspective, the additional load can cause costly power peaks and congestion in the regional electricity grid. For refineries and other

energy-intensive industries, there is also a value in consuming electricity when cost-efficient renewable electricity production is available. The concept is called demand side management (DSM) and the general definition is that an energy consumer modifies its demand for energy through variation management strategies (VMSs) to reduce the cost of energy [17]. The DSM concept can be applied to a hydrogen system by allocating the operation of the electrolyzer when there is high availability of renewable electricity production. However, there are limitations in how flexible certain hydrogen-consuming processes at refineries can be operated. To enable the electrolyzer to operate when there is available renewable electricity production, hydrogen storage can be applied to meet the hydrogen demand at all times. This variation management strategy where large volumes of energy consumption are shifted for long periods is called complementing strategy and has been proven to be cost-efficient in combination with wind variations [18]. To further increase the degree of flexibility of the hydrogen system, load shifting using batteries is considered in this thesis. Load shifting is a variation management strategy where the electric peak load is shifted in time and has been proven to be cost-efficient to manage diurnal load variations, such as solar variations.

2.2 Energy storage

For this thesis, there are two sorts of energy storages investigated, hydrogen storage and lithium-ion batteries (LIB). The different technologies offer different technological and economic characteristics. Following is a short description of the energy storages.

2.2.1 Hydrogen Storage

The large-scale storage which is in use on a worldwide scale is pressurized hydrogen tanks. The tanks are commonly manufactured in seamless steel or other materials, such as polymer (plastic) liners or composite wrapping with steel. The tanks are tested to withstand 5500 charging and discharging cycles at 125 % of nominal working pressure and are suited for long-term storage. For storing larger quantities of hydrogen gas, it is not feasible to exceed pressures of 200 bar(g) at ambient temperature, due to material limitations and costs [19].

As an alternative to pressurized hydrogen tanks, the joint venture project Hybrit aims to store hydrogen in large excavated caverns, where a pilot hydrogen storage plant in Luleå, Sweden, is up and running [20]. The technique is called lined rock cavern (LRC), where the surrounding rock formation carries the main structural load, while the steel lining creates a layer that is hardly penetrable [21]. The space between the inner steel lining and surrounding rock is filled with concrete, an illustration is seen in Figure 2.2. Hybrit sees the need to employ hydrogen storage in a full-scale hydrogen gas storage facility measuring 100,000 to 120,000 cubic meters, with a capacity to store more than 65 GWh of hydrogen gas [20]. LRC is a well-known technology and has been used to store natural gas for 20 years in the Swedish facility Skallen, Halland [21]. Skallen has a total volume of 40,000 m^3, and this translates to a capacity of 640 metric tonnes of hydrogen gas, equivalent to approximately 21 GWh of hydrogen gas [22]. Operational limitations constrain LRC storages, which in turn impact their profitability. Specifically, an LRC's maximum filling and emptying rates are subject to these limitations. Such maximum rates are determined through thermodynamic simulations, which assume that equivalent pressure changes can be tolerated when operating an LRC with hydrogen as when using natural gas [23].

According to Papadias and Ahluwalia [24], the specific investment cost for underground LRC is approximately EUR 1,900/MWh. Andersson and Grönkvist[23] show different figures, where they are estimated to be EUR 3,650/MWh. Toktarova et al. (2022) [25] are using LRC technique in their modeling, and have used even higher figures for the specific investment cost of EUR 11,000/MWh. For large-scale hydrogen storage and Swedish conditions, LRC seems to be the most cost-efficient technology for shallow depths and is fit for a variety of geological conditions [26].

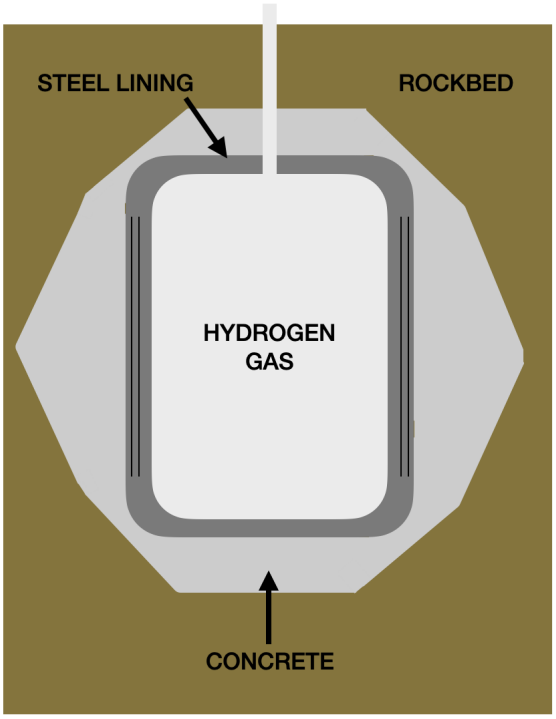

Figure 2.2: A conceptual illustration of the three layers that seal the stored hydrogen gas - rock bed, concrete, and steel lining

2.2.2 Li-ion Batteries

Lithium-ion batteries (LIB) are manufactured in small cells, which are assembled into modules that make up large packs [27]. The larger the desired storage capacity, the larger the pack. The input and output are both electricity and offer a high round-trip conversion efficiency, of approximately 90 %. There are two components that make up the round trip losses in a LIB, the operational and standby losses. Operational losses come from charging and discharging the pack and standby losses come from internal current leakage, which makes storage periods of seasonal scale for LIBs unfeasible. LIB offers a broad variety of energy system services on grid scale such as frequency and voltage regulation, and load shifting. One main design parameter of a battery is the inverse of the time to fully discharge a battery pack, the so-called C-rate. It yields a ratio between the installed capacity measured in energy and the maximum average power output from the battery. In this thesis, a C-rate of 1 is assumed, both for charging and discharging. LIBs have seen a long trend of cost decline [EUR/MWh], but recently the average prices have increased due to raw material shortage and soaring inflation [28]. Axpo will deploy a 20 MW/20MWh grid-scale battery in Sweden during 2024 [29].

One possibility with the Swedish electricity system is that it will be dominated by asynchronous and non-dispatchable generators, i.e. solar and wind power. New challenges will then arise with load balancing and frequency control and batteries seem to be promising to both short and long-term ancillary services [30]. Large-scale grid batteries can sign up as a reserve at Svenska Kraftnät (Swedish authority for power transmission), a profitable agreement [31]. With the chosen methodology of energy-only, ancillary services with batteries are delimited.

Table 2.1: Costs for energy storage technologies.

Technology	Specific investment cost [EUR/MWh]
Pressurized hydrogen tanks	45,000
Lined rock cavern	1,900-11,000
Battery	135,000

2.3 Power Purchase Agreements

A Power Purchase Agreement (PPA) is a long-term contract where an electricity consumer agrees to purchase electricity directly from an electricity producer, often to a fixed price of electricity [32]. Power purchase agreements have existed for decades in the energy industry, but the popularity of PPAs has increased due to the rapid expansion of renewable electricity production. Power purchase agreements play an important role in the electrification process of energy-intensive industries. This section aims to describe and motivate the importance of PPAs and to clarify assumptions regarding PPAs in this thesis work.

Renewable energy producers have been relying on subsidies from governments during their development phase [32]. The technical development of renewables has led to a cost reduction of renewables, which subsequently has led to the withdrawal of subsidy programs. The subsidy programs constituted as financial security for investments in renewable energy technology. The volatile electricity prices on the spot market contribute to uncertainties regarding the guarantees of the return on the investment. A power purchase agreement can provide similar financial security as a subsidy program by minimizing the risk-to-return ratio through a long-term agreement that guarantees the return on the investment. Nowadays with electricity deficits, congestion, and volatile electricity prices on the spot market, PPAs can provide security in electricity supply for consumers as well. By entering a PPA the consumer secures the supply of electricity as well as creating the incentives for new electricity generation in the system. The origin of the electricity in a PPA is known and green certificates can be obtained by entering a renewable PPA.

There are different variants of how power purchase agreements are structured, both regarding electricity supply and payment strategy [32]. The most common variant of agreement regarding electricity supply is a virtual PPA, which means that there is no physical connection between the electricity producer and consumer. The contract consists of a financial agreement enabling the consumer to purchase electricity at a certain price. In theory, the absence of a physical connection makes it possible for parties within different electricity markets and price regions to enter a virtual PPA. The other electricity supply variant of a power purchase agreement is a physical PPA, which means that there is a physical transmission connection between the producer and consumer. A physical PPA is limited to the transfer capacity between the two parties, whereas a virtual PPA is constrained by the grid connection on the consumer side. In this study, a physical PPA is assumed due to limitations in transmission capacity between the refinery and the regional grid.

The payment strategy for power purchase agreements can be structured in different ways. A baseload PPA is an agreement where the producer agrees to deliver a certain amount of electricity over a certain timeframe [32]. In return, the consumer agrees to purchase the agreed-upon volume of electricity. In a baseload PPA, the producer is responsible for covering the shaping and balancing costs. The shaping cost is the difference between the baseload price (often referred to as the average spot price) and the effective price on the day ahead spot market. In a system with a high share of renewables, the spot price is likely to be low at the time of production. This results in the cannibalization effect, where the producers cannibalize on their own income. The cannibalization effect results in shaping costs for the producers. The balancing costs stem from imbalances between the agreed-upon volume and the delivered electricity. For intermittent electricity generation, the production cannot be forecasted with full accuracy and the producer is obligated to compensate for these imbalances. The other payment strategy is called “pay-as-produced” and means that the producer has agreed on delivering a certain amount of electricity when the electricity is available

for production, e.g., during windy conditions for a wind farm [32]. The consumer agrees to purchase electricity when it is produced in time. With this payment method, the volume management and the risk associated with shaping and balancing are handled by the consumer. Typically, the producer builds a power plant or wind farm for the purpose of the PPA. This means that costs from the entire supply chain are reflected in the pricing of the PPA. In this study, a "pay-as-produced" payment strategy is assumed to avoid estimations of shaping and balancing costs and to introduce variability to the system in order to investigate flexibility measures.

Sweden is the largest market for power purchase agreements in Europe [33]. Other European countries have or have had subsidy programs like feed-in-tariffs, or capacity compensation to stimulate investments in renewable electricity capacity, whereas the relatively unregulated electricity market in Sweden has forced electricity producers to rely on other financial sources, such as power purchase agreements [34]. In the third quarter of 2020, Sweden had the lowest PPA prices for wind power in Europe. In Figure 2.3, the average PPA price can be seen in relation to the spot prices in price region SE3 during 2020. The market price for onshore wind power PPA in Sweden was 29 EUR/MWh during this year, which corresponds to the levelized cost of electricity (LCOE) for onshore wind power [33][35]. In this study, the cost of electricity via PPA is therefore assumed to be equal to the LCOE for offshore wind power.

The latest trend for power purchase agreements in Sweden is that energy-intensive industries enter long-term agreements to secure their electricity supply. The Swedish concrete producer Cementa recently entered an agreement with OX2 and the plan is to annually produce 19.5 TWh of offshore wind electricity to the upcoming concrete factory in Slite, Gotland [36]. Both Preem and ST1 have entered a partnership with Vattenfall, where the offshore wind on the west coast will contribute to the fossil-free value chain of fuel production [37] [38].

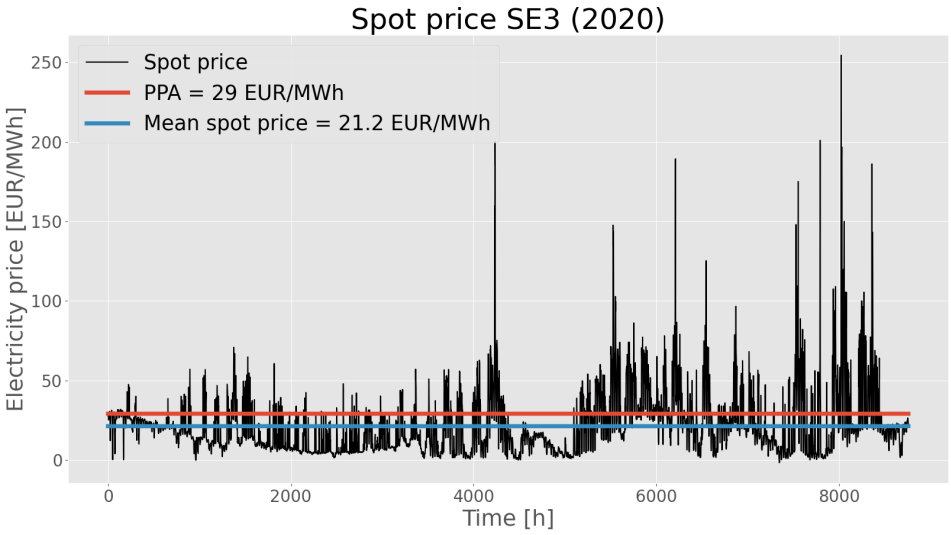

Figure 2.3: Spot prices and mean PPA price for onshore wind power in SE3 (2020).

2.4 Carbon Capture and Storage (CCS)

The employment of CCS plays a major role for Preem to reach their domestic net zero goals by the year 2035. Biermann et al. [39] state that Preem will proceed with a post-combustion amine solution unit and hence will be the only considered technology in this thesis. An amine carbon capture technology uses a circulating amine solution to extract CO_2 from the flue gas in a counter-current flow. When in contact, the carbon dioxide is absorbed from the flue gas mixture and

leaves in a concentrated stream after heat is indirectly applied with steam to strip CO_2 from the solvent. Amine post-combustion carbon capture has a capture rate of 90 % of the flue gases' total CO_2 content. Higher capture rates can be achieved but at the expense of larger heat demand. Post-combustion carbon capture is well-suited for a broad range of CO_2 sources, especially the SMR which has the highest CO_2 content in its flue gases at Preem's refinery in Lysekil. Due to the need for additional heat for operating the CCS, additional operation and maintenance costs are yielded for the site.

With the CO_2 captured, it needs to be conditioned (compression and liquefaction), transported, and stored permanently, for example beneath the seabed on Norway's west coast. These aspects do also yield further variable costs to the CCS unit.

2.5 EU Emissions Trading System (EU ETS)

The European Union have an Emission Trading System, EU ETS, which is their main policy to combat climate change and its key tool for reducing greenhouse gas (GHG) emissions cost-effectively. It covers greenhouse gases such as carbon dioxide (CO_2), nitrous oxide (N_2O), and perfluorocarbons (PFCs). It is a market designed as a "Cap and trade" system with a finite amount of allowances. The allowances are allowed to be traded within the market and therefore puts a price on the allowances [EUR/tCO_2]. All EU is included plus Iceland, Lichtenstein, and Norway. The mechanism limits GHG emissions from the energy sector, manufacturing industry, and aviation within the included countries. In total, 40 % of the EU's greenhouse gases are included in the EU ETS. Each year the number of allowances diminishes, making the supply side smaller and the price of the allowances rise [40].

3
Methods

In this section, the methodology of this thesis is presented. The hydrogen system and the linear optimization model of the hydrogen system are presented in Section 3.1. The description of the linear optimization model is followed by the methodology for economic calculations in Section 3.2, and the modeling of hydrogen storage and compression work in Section 3.3 and 3.4. A description of the sensitivity analysis is presented in Section 3.5.

3.1 The linear optimization model

In this section, the linear optimization model for minimizing the total cost of hydrogen at the refinery is presented. The minimization model consists of an objective function (Section 3.1.1), describing the total cost of hydrogen for meeting the hydrogen demand, and constraints described in Section 3.1.2, that represent technical limitations of the observed technologies and system requirements. The linear optimization model is formulated and implemented in the commercial software General Algebraic Modeling System (GAMS). The model is formulated as an investment and a dispatch model, which means that the dimensions of technologies and the operation of the technologies are optimized simultaneously, in order to minimize the total system cost. The model is on an annual basis with an hourly resolution, which allows for capturing the variability of VRE. In Figure 3.1, a system overview of the investigated hydrogen system is presented, and how the different technologies interact with each other. Note that there is no direct connection between the wind farm and the regional grid. This means that excess electricity from the offshore wind farm can only be exported to the regional grid by passing through the refinery. The transmission connection between the refinery and the regional grid is limited by the available transmission capacity. The system and technology interactions are further explained in Section 3.1.1 and Section 3.1.2. In the model, the hydrogen demand, wind profile, and electricity spot price are implemented as parameters, which provides the model with perfect foresight and yields the most cost-effective combination of technologies and operation. In Table 3.1 the notations used to describe the model are presented.

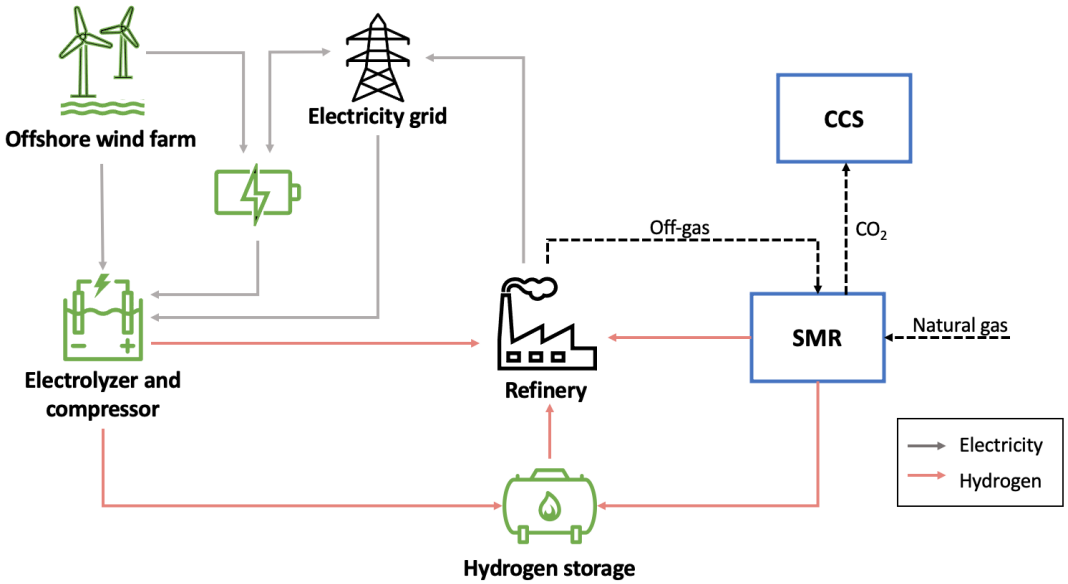

Figure 3.1: Schematic overview of the system investigated in this thesis. Technologies included in the green hydrogen system are shown in green, and technologies included in the blue hydrogen system are shown in blue.

Table 3.1: Notations describing the model.

Sets		
T	Set of time steps	{1,...,8760}
N	Set of technologies	{WF, electrolyzer, SMR, H_2 storage, battery, CCS}
$N^{storage}$	Subset of N that includes the storage technologies	{hydrogen storage, battery}
N^{H_2}	Subset of N that includes the hydrogen production technologies	{SMR, electrolyzer}
Variables		
C^{tot}	Total system cost	[EUR]
i_n	The installed capacity of technology n	[MW], [MWh]
$p_{n,t}$	Hydrogen produced by technology n at time step t	[MWh/h]
$\Delta_{n,t}$	Positive load difference of technology n between time step t and $t-1$	[MWh/h]
$s_{n,t}$	State of charge of energy storage technology n at time step t	[MWh]
$z_{s,t}^{charge}$	Charge variable for energy storage technology n at time step t	[MWh/h]
$z_{s,t}^{discharge}$	Discharge variable for energy storage technology n at time step t	[MWh/h]
e_t^{imp}	Imported electricity at time step t	[MWh/h]
e_t^{exp}	Exported electricity at time step t	[MWh/h]
Parameters		
d_t	Hydrogen demand at time step t	[MWh/h]
g_t^{wind}	Wind profile at time step t	[-]
$C_{n,t}^{op}$	Operational cost of technology n at time step t	[EUR/MWh]
C_n^{inv}	Annualized investment cost of technology n	[EUR/MW], [EUR/MWh]
C_n^{cyc}	Cycling cost of technology n	[EUR/MW]
r_n	Allowed ramping rate for hydrogen producing technology n	[-]
l_n^{min}	Minimum load for hydrogen producing technology n	[-]
q_t	Electricity spot price at time step t	[EUR/MWh]
α_n^{charge}	Maximum charge rate for energy storage technology n	[-]
$\alpha_n^{discharge}$	Maximum discharge rate for energy storage technology n	[-]
$\gamma^{transmission}$	Available transmission capacity	[MWh/h]
η_n	Conversion ratio for technology n	[-]
W	Compression work of the compressor	[MWh/MWh_{H2}]
SOC_n^{max}	Maximum storage capacity for storage technology n	[MWh]
GT	Grid tariff for power distribution	[EUR/MWh]
GP	Price of liquefied natural gas (LNG)	[EUR/MWh]
PPA	Electricity price of power purchase agreement	[EUR/MWh]
ETS	Cost for emitting CO_2 (EU Emissions Trading System)	[EUR/MWh]

3.1.1 Objective function

In Equation (3.1), the objective function for minimizing the total system cost is presented. As stated earlier, the model is an investment and a dispatch model and includes both investments in technologies and the operation of the technologies. Note that the capacity of the SMR is set to the existing SMR capacity available at the refinery, and no further investment in SMR capacity is allowed. To represent the current operation of the SMR, an additional cost (C_{smr}^{cyc}) is assigned for changing the load of the SMR, and the cost is assumed to be 2.5 EUR/MW. This is a fictive cost that mitigates fluctuating behavior of the SMR. The electricity from the offshore wind farm is bought via a physical pay-as-produced PPA, where the PPA price is estimated to be equal to the LCOE for offshore wind power. By assuming a pay-as-produced PPA, the refinery pays for all produced electricity from the offshore wind farm, even during curtailment. The model is also allowed to trade electricity with the electricity grid. Note that there is a grid tariff on the imported electricity to represent grid taxes and transmission fees. The transmission capacity between the refinery and the regional grid is limited by the existing transmission capacity at the refinery, which is explained in Section 3.1.2.

$$\begin{aligned} min\ C^{tot} = & \sum_{n \in N \setminus \{smr, wf\}} C_n^{inv} \cdot i_n + \sum_{t \in T} \Big(C_{smr,t}^{op} \cdot p_{smr,t} + C_{smr}^{cyc} \cdot \Delta_{smr,t} \Big) + \\ & + \sum_{t \in T} PPA \cdot g_t^{wind} \cdot i_{wind} + \sum_{t \in T} \Big(e_t^{imp} \cdot (q_t + GT) - q_t \cdot e_t^{exp} \Big) \end{aligned} \tag{3.1}$$

3.1.2 Model constraints

The demand constraint described in Equation (3.2) ensures that the hydrogen demand is met by the hydrogen production technologies (electrolyzer and SMR), and the hydrogen storage at all time steps. The electrolyzer technology assumed in this thesis is alkaline.

$$d_t \leq \sum_{n \in N^{H_2}} p_{n,t} - z^{charge}_{LRC,t} + z^{discharge}_{LRC,t} \ , \forall t \in T \tag{3.2}$$

The hydrogen supply from the production technologies is limited by the invested capacity i_n, according to Equation (3.3). The SMR is also subject to a constraint limiting the minimum load, Equation (3.4). The refinery is assumed to utilize off-gases as feedstock in the SMR, and the minimum load constraint simulates the utilization of these off-gases. The concept of utilizing off-gases at a refinery is explained in Section 2.1. To simplify the cost estimation for the off-gases it is assumed that the off-gases have the same marginal cost as natural gas. The electrolyzer has no constraints on minimum load and is assumed to be fully flexible within the hour. These assumptions also apply to the compressor.

$$p_{n,t} \leq i_n, \ n \in N^{H_2}, \forall t \in T \tag{3.3}$$

$$p_{smr,t} \geq l^{min}_{smr} \cdot i_{smr}, \ \forall t \in T \tag{3.4}$$

The operation of the SMR is subjected to a number of constraints that limits how fast the SMR is allowed to change the load in time. The constraints for up-ramping and down-ramping described in Equations (3.5) and (3.6) describe the technical limitations of the SMR. Equation (3.7) and (3.8) calculates the positive load difference between two time steps. The positive load difference is multiplied by the cycling cost in the objective function (Equation (3.1)) to mitigate fluctuating behavior of the SMR. The technical limitations and cycling of the SMR are described in Section 2.1.

$$p_{smr,t+1} - p_{smr,t} \leq r^{up}_{smr} \cdot i_{smr}, \ \forall t \in T \tag{3.5}$$

$$p_{smr,t} - p_{smr,t+1} \leq r^{down}_{smr} \cdot i_{smr}, \ \forall t \in T \tag{3.6}$$

$$\Delta_{smr,t} \geq p_{smr,\,t-1} - p_{smr,\,t}, \ \forall t \in T \tag{3.7}$$

$$\Delta_{smr,t} \geq p_{smr,\,t} - p_{smr,\,t-1}, \ \forall t \in T \tag{3.8}$$

The maximum capacity of hydrogen storage is assumed to be the size of the existing crude oil caverns at the refinery, which is described in Equation (3.9). There are no limitations in allowed investments in battery capacity. However, the state of charge of the energy storage is limited by the invested storage capacity, according to Equation (3.10). The state of charge for the storage technologies is presented in Equation (3.11).

$$i_{LRC} \leq SOC^{max}_{LRC} \tag{3.9}$$

$$s_{n,t} \leq i_n, \ n \in N^{storage}, \forall t \in T; \tag{3.10}$$

$$s_{n,t} = s_{n,t-1} + z_{n,t}^{charge} - z_{n,t}^{discharge},\ n \in N^{storage}, \forall t \in T \tag{3.11}$$

The following constraints relate to the operation of the energy storages. Equations (3.12) and (3.13) limit the rate of charge and discharge of the energy storages. The Equations (3.14) and (3.15) constrains the variables for charging and discharging.

$$s_{n,t+1} - s_{n,t} \leq \alpha_n^{charge} \cdot i_n,\ n \in N^{storage}, \forall t \in T \tag{3.12}$$

$$s_{n,t} - s_{n,t+1} \leq \alpha_n^{discharge} \cdot i_n,\ n \in N^{storage}, \forall t \in T \tag{3.13}$$

$$z_{n,t}^{charge} \leq \alpha_n^{charge} \cdot i_n,\ n \in N^{storage}, \forall t \in T \tag{3.14}$$

$$z_{n,t}^{discharge} \leq \alpha_n^{discharge} \cdot i_n,\ n \in N^{storage}, \forall t \in T \tag{3.15}$$

The electricity balance of the hydrogen system is presented in Equation (3.16). The equation relates the electricity-consuming technologies with the electricity supply via PPA and spot market and the utilization of battery storage. The battery efficiency is allocated on the discharge sequence to avoid double counting the energy losses. The transmission capacity between the regional grid and refinery limits the import and export of electricity, described in Equations (3.17) and (3.18).

$$(1/\eta_{electrolyzer}+W)\cdot p_{electrolyzer,t} \leq g_t^{wind} \cdot i_{wind} + e_t^{imp} - e_t^{exp} + \eta_{battery} \cdot z_{battery,t}^{discharge} - z_{battery,t}^{charge},\ \forall t \in T \tag{3.16}$$

$$e_t^{imp} \leq \gamma^{transmission},\ \forall t \in T \tag{3.17}$$

$$e_t^{exp} \leq \gamma^{transmission},\ \forall t \in T \tag{3.18}$$

To mitigate carbon dioxide emissions from the SMR, a carbon capture and storage unit (CCS) is employed. No carbon emissions are allowed except for the emissions related to the losses in the CCS unit. The CCS unit is assumed to capture 90 % of the total emissions, and the residuals escaping the CCS are accounted for through the EU ETS. The operation of the SMR is therefore limited by the capacity of the CCS unit, see Equation (3.19).

$$i_{ccs} \geq \eta_{ccs} \cdot p_{smr,t},\ \forall t \in T \tag{3.19}$$

3.2 Economic calculations for technologies

The total cost for the investigated technologies in this thesis is divided into capital expenses (CAPEX) and operational expenses (OPEX). The operational expenses can further be divided into fixed and variable operational costs. The technologies have different technical lifetimes, and the capital expenses are therefore annualized. The capital recovery factor is obtained by (3.20), where i is the interest rate and n is the technical lifetime of the component. The interest rate used in this thesis is 5%. The annualized investment i_n, $n \in N$ where N is the technologies investigated, including fixed operating and maintenance costs on a yearly basis, are obtained by Equation (3.21), where CAPEX is measured in [EUR/MW] and fixed operational and maintenance costs are

measured in [EUR/MW/yr]. For energy storage technologies CAPEX is measured in [EUR/MWh] and fixed operational and maintenance costs are measured in [EUR/MWh/yr].

$$r = \frac{i\,(i+1)^n}{(1+i)^n - 1} \tag{3.20}$$

$$i_n = r \cdot \text{CAPEX}_n + \text{fixed O\&M}_n \tag{3.21}$$

3.2.1 Operational cost of SMR

The total operational and maintenance cost of the SMR, C^{op}_{smr} [EUR/MWh$_{H2}$], is determined by three parameters - gas price, OPEX of the CCS and the EU ETS allowance price. The costs arising from the CCS are multiplied by the ratio of metric tonnes of CO_2 released for producing 1 MWh of hydrogen gas in the SMR, which is estimated to be 0.28 [mt/MWh] [41]. Operational expenses C^{op}_{ccs} for CCS are presented in Appendix A and were provided by Preem.

$$C^{op}_{smr} = \frac{\text{gas price}}{\eta_{smr}} + 0.28 \cdot (C^{op}_{ccs} + (1 - \eta_{ccs}) \cdot ETS) \tag{3.22}$$

3.2.2 Levelized Cost of Hydrogen

The levelized cost of hydrogen (LCOH) describes the average cost of producing 1 MWh of hydrogen. The blue and green hydrogen system costs are distinguished with two different LCOH, where their respective average costs are determined. $LCOH_{blue}$, describing the average cost of hydrogen produced of the SMR with employed CCS unit, is computed in Equation (3.23). The levelized cost for the green system $LCOH_{green}$, constituting of running costs for PPA, export and import, and investments in electrolyzer and energy storages, is computed in Equation (3.24). The total levelized cost of hydrogen is computed as the weighted average of the green and blue system, according to Equation (3.25).

$$LCOH_{blue} = \frac{\sum_{t \in T} C^{op}_{smr,t} \cdot p_{smr,t}}{\sum_{t \in T} p_{smr,t}} \tag{3.23}$$

$$LCOH_{green} = \frac{C^{inv}_{elec} \cdot i_{elec} + \sum_{n \in N^{storage}} C^{inv}_{n} \cdot i_n + \sum_{t \in T} PPA \cdot g^{wind}_t \cdot i_{wind} + \sum_{t \in T} e^{imp}_t (q_t + GT) - q_t \cdot e^{exp}_t}{\sum_{t \in T} p_{elec,t}} \tag{3.24}$$

$$LCOH = \frac{LCOH_{green} \sum_{t \in T} p_{elec,t} + LCOH_{blue} \sum_{t \in T} p_{smr,t}}{\sum_{n \in N^{H_2}} \sum_{t \in T} p_{n,t}} \tag{3.25}$$

3.2.3 Levelized cost of offshore wind power

The levelized cost of electricity (LCOE) for the offshore wind farm describes the average cost of producing 1 MWh of electricity. The LCOE is affected by the annualized capital expenses C^{inv}_{wf}, the operational expenses C^{op}_{wf}, and the full load hours (FLH) of the wind profile. An average FLH is determined from ten different wind profiles for the years 2010-2019. The wind profiles are generated by GlobalEneryGIS [42], see Section 3.5.5. The levelized cost of electricity for the offshore wind farm is presented in Equation (3.26). As mentioned in Section 3.1.1, the PPA price is estimated to be equal to the LCOE of offshore wind power.

$$LCOE = \frac{C^{inv}_{wf} + C^{op}_{wf} \cdot FLH}{FLH} \tag{3.26}$$

3.3 Compression of hydrogen

Hydrogen is a lightweight gas in ambient conditions with high energy content per mass unit (33 kWh/kg$_{H2}$), but has low volumetric energy content (2.8 kWh/Nm^3). To cost-efficiently store hydrogen, it is common to compress it mechanically with compressors, even if the ambient pressure of the hydrogen gas is acceptable for end-use. The desired hydrogen pressure level at refineries depends on the design of the refinery and the technical requirements for hydrogen-consuming processes. The hydrogen pressure level assumed in this thesis is 80 bar, which approximately corresponds to the pressure level at Preem's refineries. The operating pressure assumed for the alkaline electrolyzer is 3 bar(g) (p_1), and the mechanical work needed to compress hydrogen from p_1 to desired pressure p_2 can be described with the Equations (3.27)-(3.30). For an adiabatic process, the new temperature T_2 [K] is obtained with Equation (3.27).

$$T_2 = T_1 \left(\frac{p_2}{p_1}\right)^{(\gamma-1)/\gamma} \tag{3.27}$$

The enthalpy [kJ/kg] of an ideal gas can be expressed as in Equation (3.28).

$$h = C_p T \tag{3.28}$$

The work [kJ/kg] of an ideal gas over a turbomachine is determined by Equation (3.29).

$$\Delta w = h_2 - h_1 = C_p(T_2 - T_1) \tag{3.29}$$

The ideal compression work, W [MWh/MWh$_{H2}$] for hydrogen can then be expressed according to Equation (3.30).

$$W = C_p(T2 - T_1) \cdot 3.6 \cdot 10^{-3} \cdot \rho_e^{-1} \tag{3.30}$$

3.4 Sizing of hydrogen storage

In reality, the existing space to build LRC is limited to existing crude oil caverns on site. An upper limit for investments in LRC is therefore determined using the ideal gas law. The volume V [m^3] is given by the existing volume of the crude oil caverns, assuming temperature T [K] and the desired storage pressure p_2 [Pa]. The ideal gas constant R=8.314 [J/mol/K] and the molar mass of hydrogen M [kg/mol], yields a mass that is converted to the energy quantity [MWh] according to Equation (3.31).

$$SOC_{max} = \frac{p_2 V}{T}\frac{M}{R} \cdot \rho_e \tag{3.31}$$

3.5 Sensitivity Analysis

To identify sensitive system parameters and analyze how these affect the cost-optimal system configuration, a sensitivity analysis has been carried out. The uncertainty for certain system parameters also motivates a sensitivity analysis. The sensitivity analysis was conducted by changing the value of a specific parameter and comparing the results with a reference. In the sensitivity analysis, one parameter is changed at a time to be able to quantify the impact on the system. The parameters investigated in the sensitivity analysis are - the cost of offshore wind power (PPA), the specific investment cost of hydrogen storage, transmission capacity, spot price data, the operational expenses for the SMR, and finally wind profiles from different years. Financial figures, technical lifetimes, and efficiencies for the respective technology used in the reference case are presented in Appendix A. In the reference case, a wind profile and electricity spot prices are used from the year 2019.

3.5.1 The cost of offshore wind power

Power purchase agreements are established contracts used in industry and by utility companies. The popularity of these types of agreements is fast-growing with the rapid implementation of renewable energy. In this thesis, a PPA cost of 53 EUR/MWh is used as a reference. The PPA cost is determined by the levelized cost of electricity for offshore wind power described in Equation (3.26). To account for uncertainties related to PPA costs, a sensitivity analysis was conducted that involved changing the cost of PPA in the range of 42-85 EUR/MWh.

3.5.2 The investment cost of hydrogen storage

According to previous studies, hydrogen storage enables to manage variations of VRE and supports a constant supply of hydrogen. The literature shows a broad span of the investment cost for hydrogen storage [19][24][23][25]. Therefore, a sensitivity analysis of the specific investment cost of hydrogen storage has been conducted. The assumed investment costs in the sensitivity analysis represent both lined rock caverns and pressurized hydrogen tanks, in the range of 1,900-45,000 EUR/MWh (see Table 2.1). The absence of hydrogen storage is also investigated in this sensitivity analysis, where no investment in hydrogen storage is allowed.

3.5.3 Transmission capacity and forecasted spot prices

The transmission capacity between the regional grid and the refinery limits electricity import and export. The future transmission capacities for Preem's refineries are uncertain and are therefore included in the sensitivity analysis. The transmission capacity between the regional grid and the refinery is varied between 0-60 MW to investigate the impact on the hydrogen system. In the model, the transmission capacity is implemented as a parameter and no investment costs are considered. Note that electricity supply outside the system boundary (Figure 3.1) is not considered and it is assumed that electricity imported from the regional grid has no effect on the marginal cost of electricity production. In the case where no transmission capacity is assumed, the refinery is in "island mode" with no ability to import and export electricity. In that case, the hydrogen system relies solely on the electricity supply from the offshore wind farm.

The electricity spot price is implemented as a parameter in the model from historic data. In the near future, the electricity spot market is expected to fluctuate more when introducing more renewable electricity generation. As a reference, the spot prices for 2019 have been used in this thesis. To investigate how a higher share of renewable electricity generation affects the model, the forecasted marginal cost of electricity production for 2050 is used. The marginal cost of electricity generation is assumed to be equal to the spot price that would be sold on the spot price market and is henceforth referred to as spot prices. The forecasted spot prices of 2050 are tested with different transmission capacities in the range of 0-60 MW. The forecasted spot prices for 2050 were generated by Öberg, Odenberger, and Johnsson [43] with the cost-minimizing electricity system investment model eNODE. The model minimizes the total costs of necessary investments and operation of the system to meet electricity and hydrogen demand for a future European energy system assuming zero emissions of carbon dioxide. The forecasted spot price data is generated for a combined region of bidding areas SE3 and SE4. eNODE uses technology data such as efficiencies, fuels, operational expenses, and weather profiles to generate total system costs, dispatch profiles, and marginal costs for electricity generation. The forecasted share of installed capacity for year 2050 for different technologies are generated by [43], and the reference values for Swedish electricity mix are obtained from [44], all seen in Figure 3.2. Originally, eNODE was developed by Göransson et al. [45].

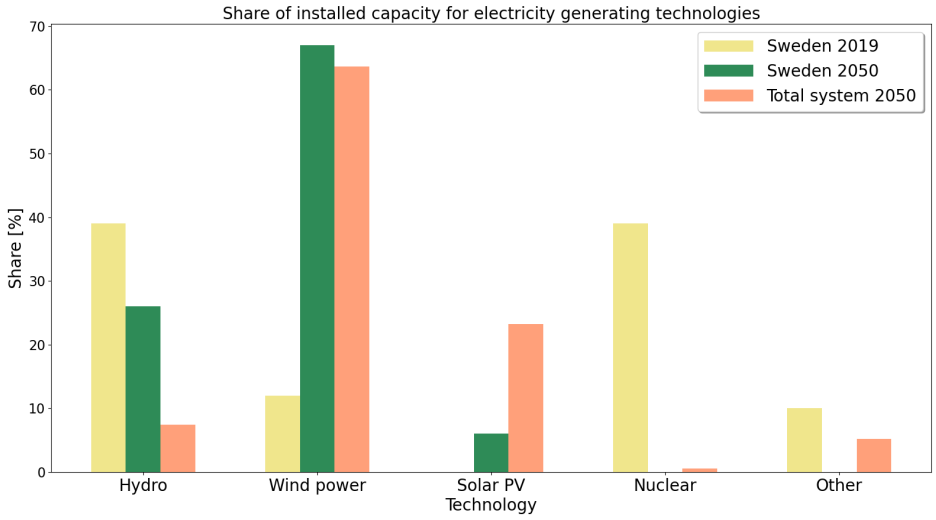

Figure 3.2: The share of installed capacity of electricity generating technologies for Sweden 2019, Sweden 2050, and the total system 2050.

3.5.4 Operational cost of the SMR

The operational and maintenance cost of the SMR, C^{op}_{smr}, is determined by Equation (3.22), which is depending on three parameters: OPEX of the CCS unit, gas price, and EU ETS. The two latter are decided on spot markets and are therefore associated with uncertainties. The fact that the SMR is assumed to utilize off-gases as feedstock also contributes to uncertainties regarding the operational cost of the SMR. As stated earlier, the amount of available off-gases at the refinery is a consequence of refinery design and the market value of different types of fuels and chemicals, and the off-gases are assumed to have the same marginal cost as natural gas.

Throughout the year 2022, European prices of liquefied natural gas (LNG) increased drastically and reached an all-time high at the Dutch LNG market Title Transfer Facility, measuring 345 EUR/MWh [46]. This can be compared to the average of 22.5 EUR/MWh during the period of 2010-2019 [47], an increase of more than 1400 %. With elevated inventories, an overall lower gas consumption compared to historical levels and a mild winter in the EU has made the spot price to find a new average of 55 EUR/MWh for the first three months of 2023 [48]. As a reference value of gas prices for the sensitivity analysis, a five-year average of the Dutch TTF market is estimated to be 57.4 EUR/MWh, measuring from February 2023 and five years back [46].

The EU ETS allowance prices have seen a drastic increase recently, with a large uncertainty ahead. On February 20th, EU ETS did breach the 100 EUR/tCO_2 mark for the first time [49] and forecasts estimate prices of 160 EUR/tCO_2 by the year 2030 [50]. As a reference value of the EU ETS allowance price, 100 EUR/tCO_2 is assumed in the reference case. This yields a reference value to the operational expenses to the SMR equivalent to 110 EUR/MWh$_{H2}$ and the sensitivity analysis will be carried out for values in a range of 55-165 EUR/MWh$_{H2}$, representing the operational cost of the SMR.

3.5.5 Wind profiles

The wind profiles used in the model are generated by Mattsson, Verendal, Hedenus, and Reichenberg's model GlobalEnergyGis [42]. GlobalEnergyGIS generates normalized supply curves for different VREs for arbitrary regions of the world using a reanalysis of geospatial datasets. The GIS model uses a mesh grid, with the size of approximately 1 km^2 for offshore wind power, where employment of wind farms is enabled 5 kilometers from the coastal strip and at shallow waters

(waters more shallow than 40 meters). The wind profiles are generated over a region covering the coast of the municipalities Lysekil, Uddevalla, Orust, Tjörn, Stenungsund, Kungälv, Öckerö, and Gothenburg. This region yields a geographical smoothing to GIS' wind profiles compared to what an individual offshore wind farm would have, mitigating the variability, suppressing large derivatives of load, and providing a higher capacity factor. The reference case is carried out for 2019 and the sensitivity analysis is conducted for the years 2015-2018. Since electricity spot price is interlinked with weather data, spot prices from the associated year are used in respective optimization for bidding area SE3.

This sensitivity analysis aims to give indications of whether the model is sensitive to one given wind profile isolated to one year. Therefore all wind profiles are analyzed individually and with one consecutive model run covering the years 2015-2019 with associating spot price data. To differentiate between different years' wind profiles, two parameters are used. To start with, the capacity factor CF is determined according to Equation (3.32), which describes the ratio of actual normalized energy output compared to the theoretical over a year.

$$CF = \sum_{t \in T} g_t^{wind} / 8760 \tag{3.32}$$

Secondly, the dimensioning time period is used. This is defined as the time step $t_{full} \in T$ when the hydrogen storage is full until the time step t_{empty}, where the storage is entirely emptied. With consecutive wind profiles over multiple years, this concept is extended to cycling of the hydrogen storage. One cycle is measured as when the storage is fully charged, discharged, and charged again.

4
Results

In this section, the results are presented and visualized. In Section 4.1 the results from the reference case are presented, and is followed by the sensitivity analysis in Section 4.2. Financial figures, technical lifetimes, and efficiencies are presented in Appendix A, and numerical figures for parameters are shown in Appendix B.

4.1 Reference case

The resulting total annualized system cost for the reference case is 374 million euros. In the reference case, 60% of the demand is supplied by the SMR, and the remaining 40% of the demand is met by the electrolyzer. In Table 4.1, the numerical results for the reference case are presented. The green hydrogen system consists of a 263 MW_{H2} electrolyzer, 14 GWh of hydrogen storage, and 2.3 MWh of battery capacity. The optimization model invests in a CCS unit with a CO_2 capture rate of 83.6 tonne CO_2/h. These investments do altogether yield an investment cost of approximately 444 million euros. The cost-optimal wind farm capacity in the reference case is 469 MW. The produced electricity from the wind farm is 2109 GWh during the year, whereas the electrolyzer consumes 2096 GWh of electricity. There is a surplus of electricity in the system, which contributes to 2.9 GWh of curtailment. The model exports 20.5 GWh and imports 10.9 GWh of electricity. The capacity factors for the hydrogen production technologies are 56.9 % and 76.4 % for the electrolyzer and the SMR, respectively. The combined levelized cost of hydrogen is 113.4 EUR/MWh_{H2}. The levelized cost of hydrogen for the green system is 111.0 EUR/MWh_{H2} and 115.0 EUR/MWh_{H2} for the blue system. The marginal cost of hydrogen production describes the cost of producing one extra unit of hydrogen. The maximum marginal cost is obtained during hours with low wind power output and maximum load of the SMR and results in 363 EUR/MWh_{H2}. The average marginal cost of hydrogen production is 122 EUR/MWh_{H2}, slightly higher compared to the OPEX of SMR, being 110 EUR/MWh_{H2}.

Table 4.1: Numerical results for the reference case.

Type					
Installed capacities	**Electrolyzer** [MW_{H2}] 263	**Wind farm** [MW] 469	**LRC** [GWh] 14	**Battery** [MWh] 2.3	
Operation	**Electrolyzer consumption** [GWh_{el}] 2096	**Wind farm** [GWh_{el}] 2109	**Curtailment** [GWh_{el}] 2.9	**Export** [GWh_{el}] 20.5	**Import** [GWh_{el}] 10.9
Capcaity factors	**Electrolyzer** 56.9 %	**SMR** 76.4 %			
Levelized cost of hydrogen	**Hydrogen** [EUR/MWh] 113.4	**Green hydrogen** [EUR/MWh] 111.0	**Blue hydrogen** [EUR/MWh] 115.0		

The two largest expenses of the total annual system cost are related to operational costs, where 58.3 % are dedicated to the SMR and 30.2 % to the purchase of PPA. An illustration of the distribution of all costs is shown in Figure 4.1. Altogether, the investment costs account for 11.1% of the total system cost. The electricity import accounts for 0.4% of the total system cost, and the investment cost for the battery is negligible.

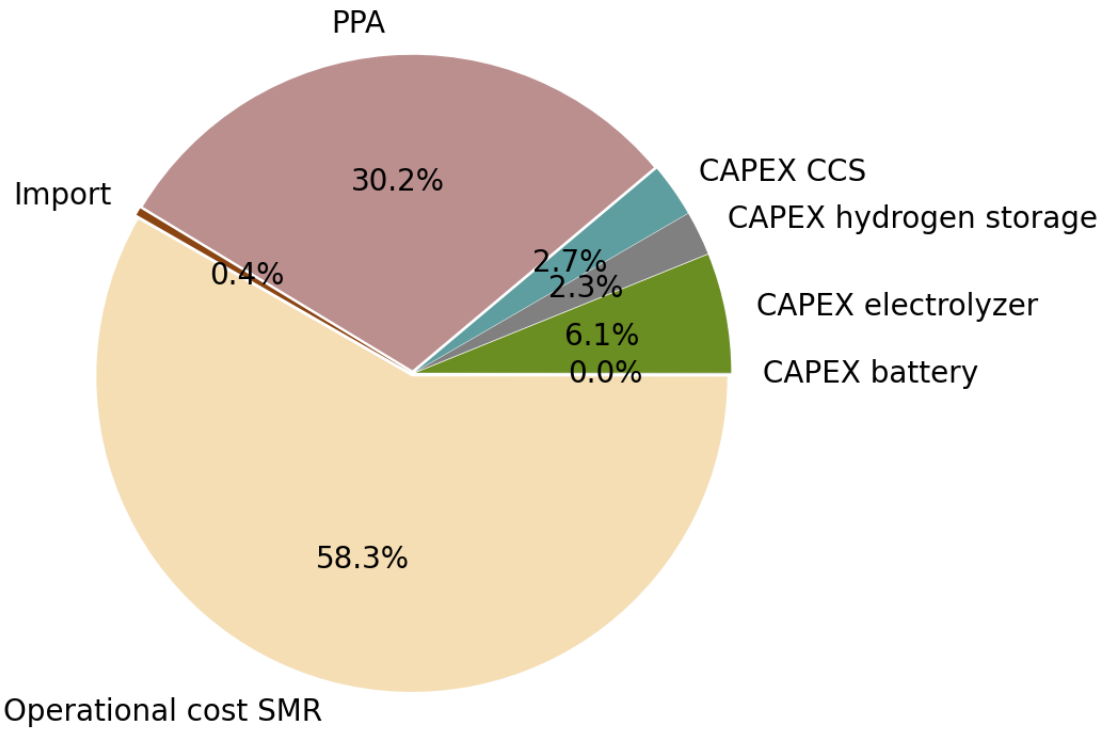

Figure 4.1: Distribution of costs for the hydrogen system. Note that *PPA*, *import* and *operational cost of the SMR* are related to the operational expenses of the hydrogen system. The capital expenses are annualized according to Equation (3.21).

In Figure 4.2a, the hydrogen supply and demand during arbitrary 1500 hours can be seen. The constant hydrogen demand of 377 MWh_{H2}/h is met by the electrolyzer, SMR, and discharge of the hydrogen storage. During hours with a surplus of hydrogen production, the storage is charged. Surplus production is mostly due to high wind power output from the offshore wind farm. For some hours the SMR contributes to charging the hydrogen storage, this is a result of the ramping constraint on the SMR. During high wind power output, the SMR is operated on part load. The results show that the SMR is operated on minimum load during longer periods with high wind power output.

In Figure 4.2b, the electricity production from the offshore wind farm and the electricity consumption for the green system are presented. The electrolyzer electricity consumption and charge of the battery follow the wind profile, but there are hours when the wind output exceeds the electricity consumption. During these hours with excess electricity in the hydrogen system, curtailment occurs. There are also occasions when the electricity consumption exceeds the wind power output. During these occasions, electricity is imported from the regional grid.

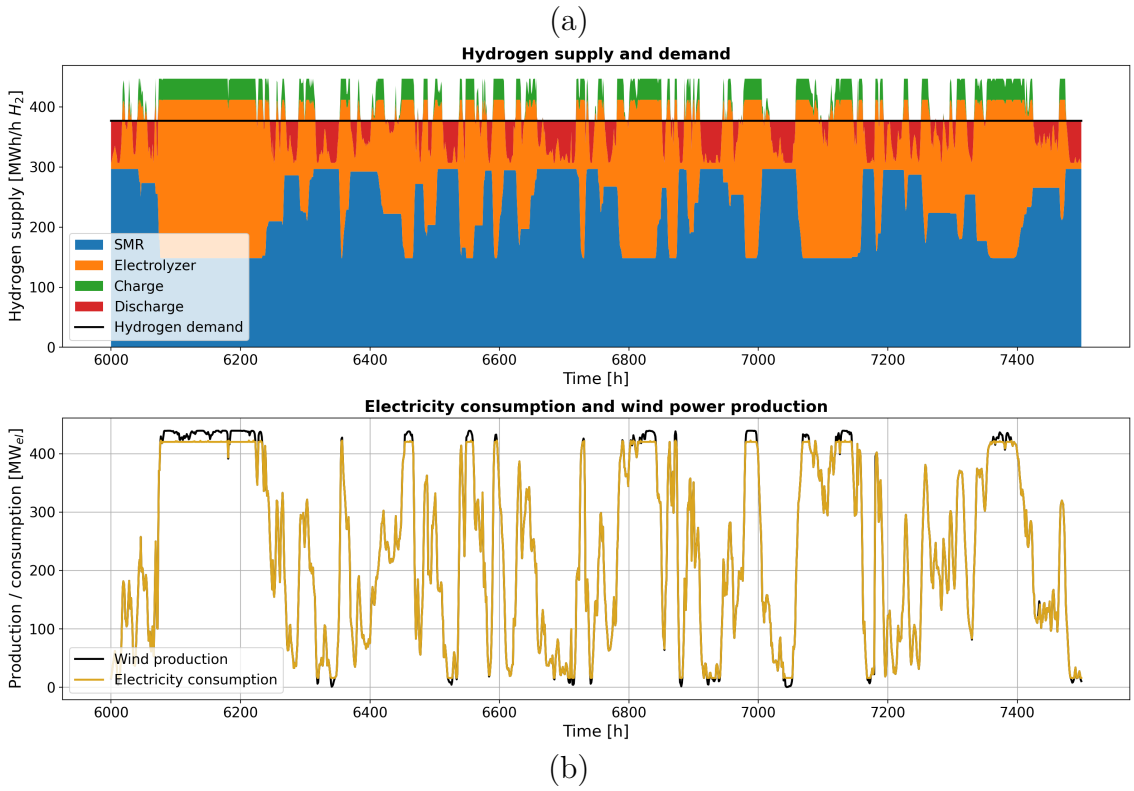

Figure 4.2: Hydrogen supply from the electrolyzer, SMR and hydrogen storage, and the hydrogen demand for 1500 arbitrary hours (a). The wind power production from the offshore wind farm and the electricity consumption of the electrolyzer (b).

In Figure 4.3 the state of charge for the hydrogen storage is presented for 8760 hours. The state of charge starts and ends at the same level of 6.2 GWh. The storage is full (14.0 GWh) two times during the year, which occurs around hours 2,100 and 4,500. During the time period between hours 4,500-5,300, the storage is completely discharged. This period where the state of charge goes from full to empty is considered as the dimensioning time period. The dimensioning time period determines the hydrogen storage capacity.

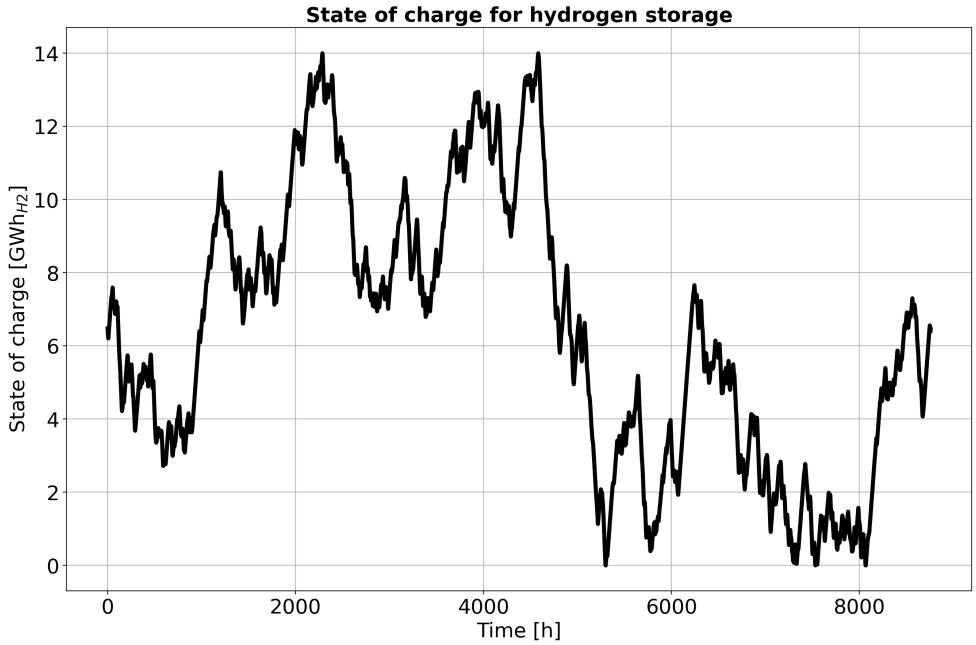

Figure 4.3: State of charge for the hydrogen storage during the time set of 8760 hours. The storage capacity is dimensioned by the time period between hours 4,500 and 5,300, where the state of charge goes from full to empty.

In Figure 4.4a-c, the operation of the battery, electricity trading, electrolyzer electricity consumption, and wind power output can be seen for 200 arbitrary selected hours. Interesting about these results is that the model uses import to increase the capacity factor for the electrolyzer. This can be seen in Figure 4.4c, where the electrolyzer consumption exceeds the wind power output from the wind farm between hours 5240-5300. For the same time period, the model imports electricity to increase the load of the electrolyzer (Figure 4.4b). Between hours 5320-5360, the electrolyzer is operated at full capacity and the wind power output from the wind farm exceeds the consumed electricity in the electrolyzer. During these hours the model exports electricity to the regional grid. Similar behavior can be observed for the operation of the battery, where the battery is discharged to increase the load of the electrolyzer, especially during periods with low or no import. The charging of the battery storage occurs during import or when there is an overproduction of wind power from the wind farm.

Figure 4.4: Battery charge and discharge (a), electricity import and export (b), electrolyzer electricity consumption and wind power production (c).

4.2 Sensitivity Analysis

The robustness of the model is analyzed with the sensitivity analysis. In this section, the results of the sensitivity analysis described in the method (Section 3.5) are presented. The analysis is in relation to the reference case described in Section 4.1.

4.2.1 The cost of offshore wind power

In Figure 4.5a, the total system cost in relation to the reference case is presented for different costs of offshore wind (PPA). The PPA is in the range of 42-85 EUR/MWh, where the reference value of the PPA is set to 53 EUR/MWh. The cost of offshore wind power affects the total system cost, where a lower price of the PPA, yields a reduction of the total system cost, compared to the reference value. With a PPA of 42 EUR/MWh, the total system cost decreased by 6.2 %, and with a PPA of 85 EUR/MWh, the total system cost increased by 13 % compared to the total cost of the reference case (374 MEUR/yr). The model is constrained in SMR capacity and electricity transmission capacity and is therefore relying on electricity from the offshore wind farm to meet the hydrogen demand. This is why the total system cost increases with the increasing cost of offshore wind power.

The levelized cost of hydrogen is also affected by the cost of offshore wind power. The reference case yields a total levelized cost of 113.4 EUR/MWh$_{H2}$, whereas the levelized cost for the green and blue systems is 111.0 EUR/MWh$_{H2}$ and 115.0 EUR/MWh$_{H2}$, respectively. In Figure 4.5b, the levelized cost of hydrogen is presented for different costs of offshore wind power, where it varies proportionally with the value of PPA in the price range 94.2-177.1 EUR/MWh$_{H2}$. The figure shows the levelized cost for the green and blue systems, where the respective cost contributions are shown. The total levelized cost of hydrogen is a weighted average of the blue and green system, calculated with Equation (3.23) and (3.24). The levelized cost for the blue system is not affected by the cost of offshore wind power. For the green system, the cost contributions for offshore wind power, imported electricity from the grid, and investment in hydrogen storage causes the levelized

cost to increase.

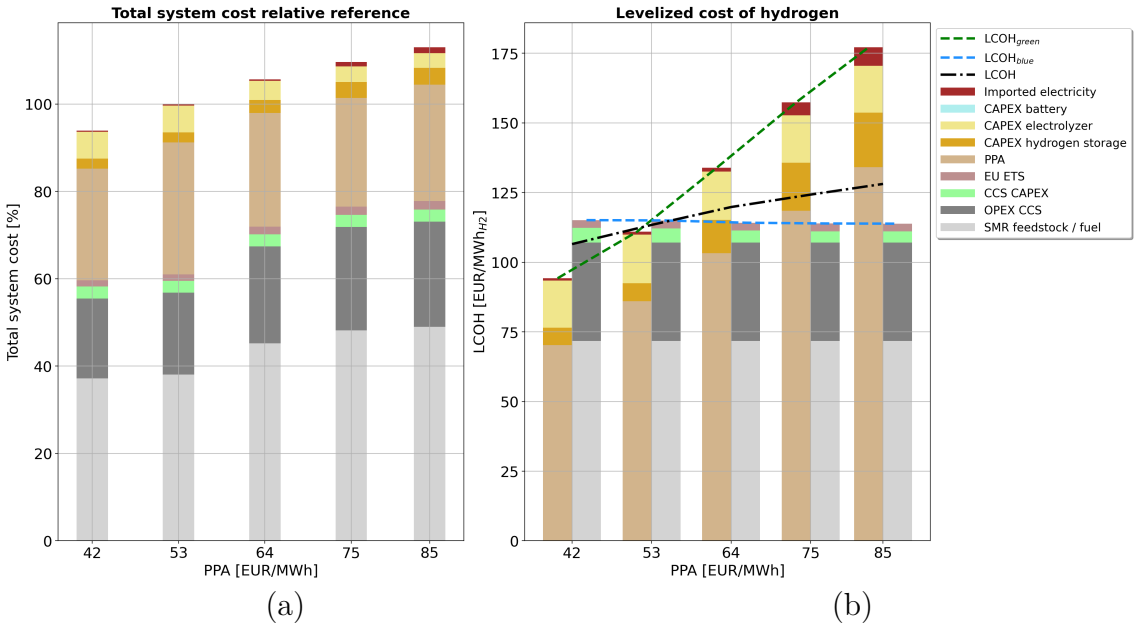

(a) (b)

Figure 4.5: Total system cost in relation to the reference case (a), and levelized cost of hydrogen for different costs of offshore wind power (b).

In Figure 4.6a, the electrolyzer capacity and offshore wind farm capacity are presented for different costs of offshore wind power. The results show a reduction of invested electrolyzer and wind farm capacity with increasing costs for offshore wind power. The cost of offshore wind power is modeled as a pay-as-produced PPA, which means that all electricity produced from the offshore wind farm is transmitted to the refinery. The refinery is therefore obligated to pay for electricity when electricity is produced on time, even during curtailment. This results in less wind farm and electrolyzer capacity when the PPA cost increases.

Similar reasoning can be applied when analyzing the hydrogen storage capacity for different PPAs in Figure 4.6b. When the cost of offshore electricity increases, the model favors a larger storage capacity for hydrogen to manage a smaller electrolyzer and offshore wind farm. However, the battery storage capacity decreases with increasing PPA costs. The difference between wind farm capacity and electrolyzer capacity, seen in Figure 4.6a, decreases with increasing PPA cost. The battery storage utilizes the excess electricity not consumed by the electrolyzer, and with a smaller difference between the wind farm and electrolyzer capacity, there is less excess electricity available for the battery storage. Therefore, the battery capacity is 0 MWh for PPA costs of 64 EUR/MWh or above.

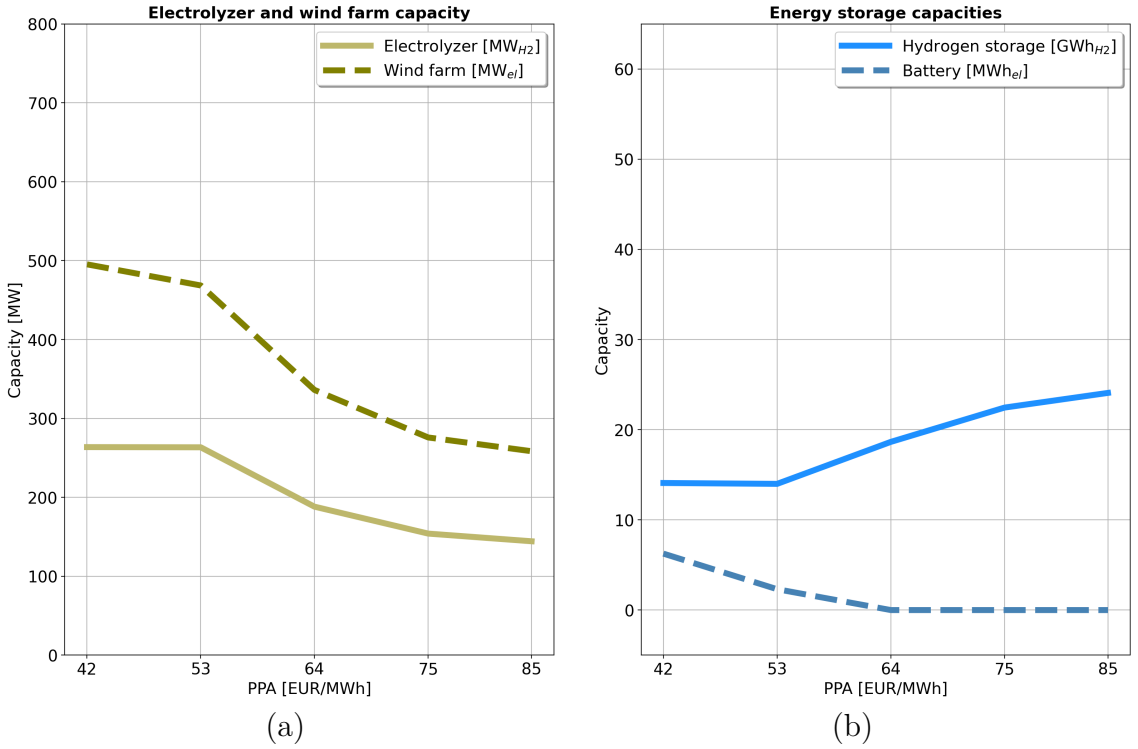

Figure 4.6: Electrolyzer and wind farm capacities for different costs of offshore wind power (a). Hydrogen storage and battery storage capacities for different costs of offshore wind power (b). Note that energy storage capacities are given in different magnitudes. Hydrogen storage capacity is given in GWh and battery storage capacity is given in MWh. The reference cost of offshore wind power (PPA) is 53 EUR/MWh.

In Figure 4.7a, the annual hydrogen production from the hydrogen production technologies for different PPAs is presented. For PPA costs in the range of 42-85 EUR/MWh the SMR stands for a majority of the hydrogen supply to the refinery. The hydrogen supply from the SMR steadily increases with increasing costs of PPA, whereas the supply from the electrolyzer decreases for the same range of PPA costs. This trend corresponds with the results shown in 4.5b, where the levelized cost of hydrogen is presented. The LCOH for the green system increases, while the LCOH for the blue system remains constant with increasing costs of PPA. It is therefore more cost-efficient to meet the majority of the hydrogen demand with the SMR. The same trend is seen in Figure 4.7b, where the capacity factors for the hydrogen production technologies are shown. The capacity factor for the SMR increases with increasing costs of PPA and reaches a capacity factor of 98.4% with a PPA of 85 EUR/MWh. This can be compared with the reference case which yielded a capacity factor of 76.4% for the SMR with a PPA of 53 EUR/MWh. Note that no further investment in SMR capacity is allowed, which means that the SMR capacity factor is directly correlated with the hydrogen supplied by the SMR. This is not the case for the electrolyzer, where the installed electrolyzer capacity varies with different costs of PPA.

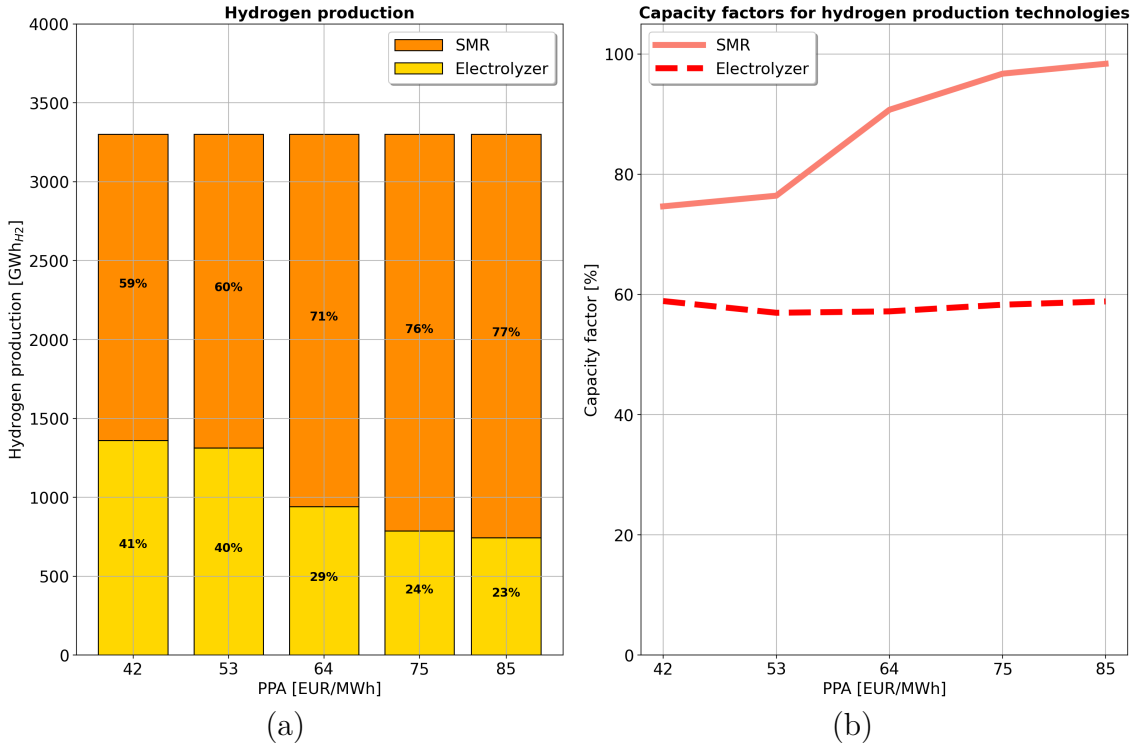

Figure 4.7: The annual hydrogen production from the hydrogen production technologies (SMR and electrolyzer) (a). Capacity factors for each hydrogen production technology (b).

Electricity import, export, and curtailment with different PPA costs are shown in Figure 4.8. In the reference case with a PPA of 53 EUR/MWh, 10.9 GWh of electricity is imported from the regional grid, whereas 20.5 GWh is exported from the refinery. With a PPA cost above 70 EUR/MWh, the model favors the import of electricity, rather than export from the refinery. The trend observed for the import is similar to the trend seen for the hydrogen storage capacity presented in Figure 4.6b. The curtailment for the reference case is 2.9 GWh and it decreases with increasing PPA costs. This trend corresponds to the results observed for the electrolyzer and wind farm capacities, seen in Figure 4.6a. As stated earlier, the difference between wind farm capacity and electrolyzer capacity decreases with increasing PPA cost, which results in less overproduction of electricity, hence less curtailment.

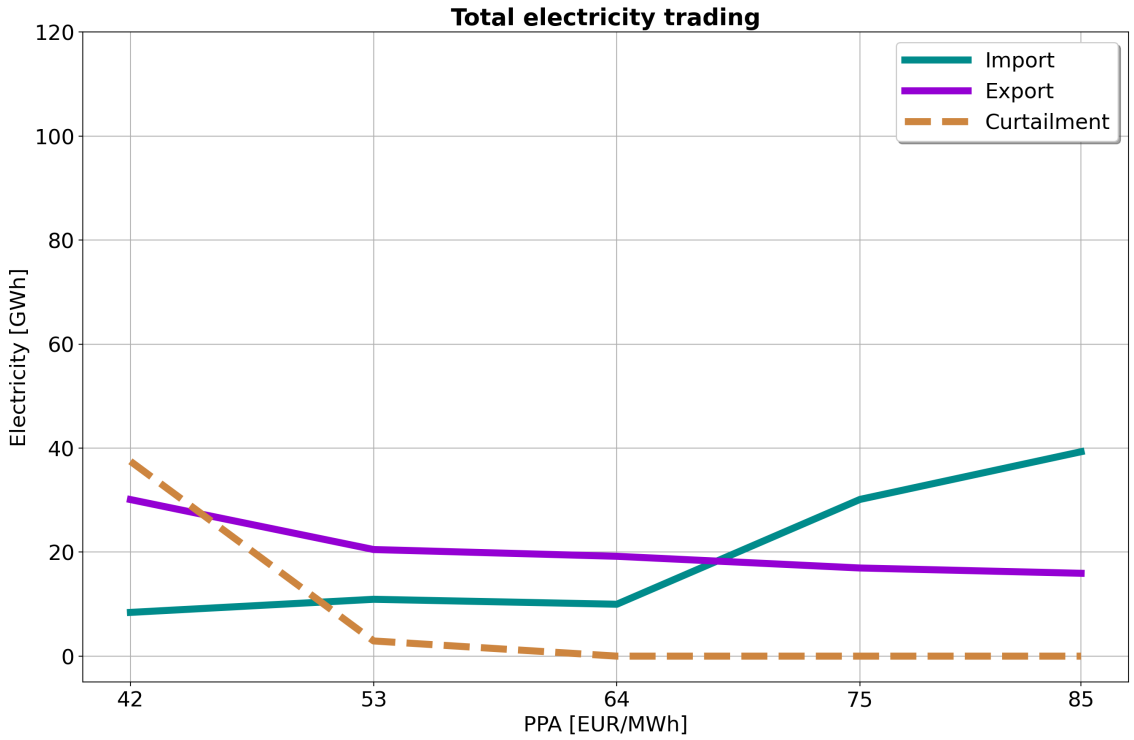

Figure 4.8: Electricity trading with different PPA costs. Included in the trading is electricity import and export, and the curtailment that is a result of excess electricity from the offshore wind farm that cannot be utilized or exported due to model constraints.

4.2.2 The investment cost of hydrogen storage

Figure 4.9a shows how the relative total system cost changes with different specific investment costs for hydrogen storage and the total system cost for a system with no available hydrogen storage. Note that the results of this section are plotted as bars since the x-axis is discontinuous. Over the whole test range, the total system cost increases with the specific investment cost of hydrogen storage and continues to increase with disabled hydrogen storage. With a specific investment cost of 1,900 EUR/MWh for hydrogen storage, the system becomes 2.6 % lower compared to the reference case. With a specific investment cost of 45,000 EUR/MWh for hydrogen storage, representing the cost of pressurized hydrogen tanks, the total system cost becomes 6.8 % more expensive compared to the reference case. With the disabled possibility to invest in hydrogen storage, the system becomes 25.9 % more expensive. Figure 4.9b shows the LCOH for different specific investment costs of hydrogen storage. The change in LCOH for the blue system is negligible over the price range. The green system becomes cheaper with a lower specific investment cost for hydrogen storage. With a specific investment cost of 1,900 for hydrogen storage, the resulting LCOH of the green system is 107 EUR/MWh, which is 3.5 % lower compared to the reference case. With a specific investment cost of 45,000 EUR/MWh, representing pressurized hydrogen tanks, the resulting LCOH of the green system is 130 EUR/MWh, which is 18.2 % higher compared to the reference case with assumed lined rock cavern to a cost of 11,000 EUR/MWh. With no available hydrogen storage, the resulting LCOH for the green hydrogen system is 170 EUR/MWh, 53.0 % higher compared to the reference case.

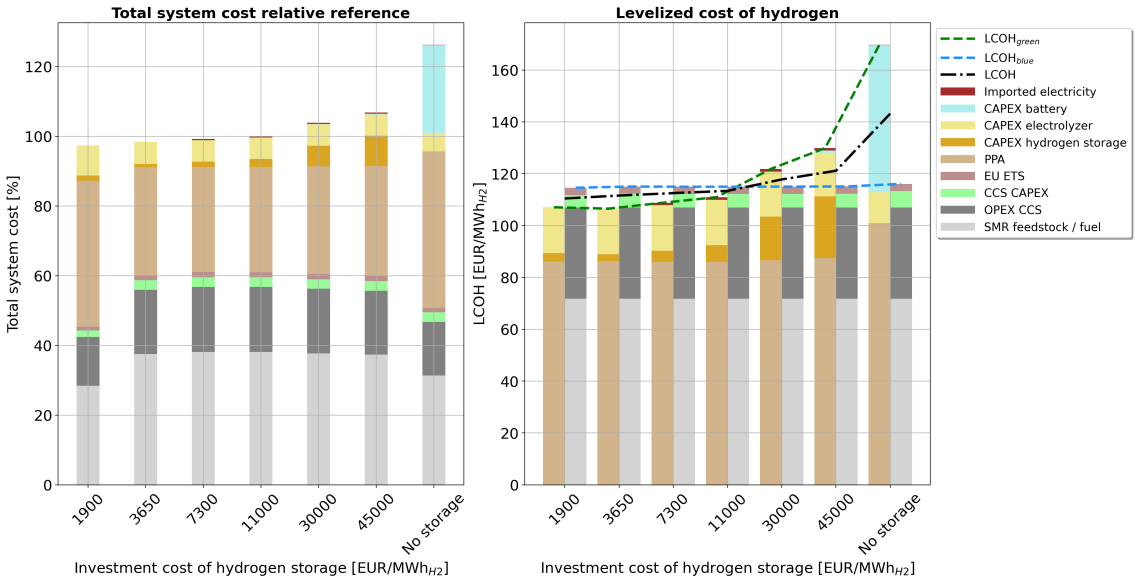

(a) (b)

Figure 4.9: The relative change of total system cost (a), and LCOH for the green and blue hydrogen system (b).

The different specific investment cost for hydrogen storage does affect both electrolyzer and wind farm capacity, but the two technologies do not follow the same trend as seen in Figure 4.10a. The electrolyzer has its largest capacity (370 MW_{H2}) for the lowest specific investment cost and a more stable segment for the other investment cost, steadily decreasing from 271 MW_{H2} to 261 MW_{H2} with rising storage costs. With no available hydrogen storage, the resulting electrolyzer has a capacity of 228 MW_{H2}. The wind farm capacity follows more of a parabolic trend, with a large start (649 MW) and end capacity (697 MW) and a stable segment around 480 MW. For a low specific cost of hydrogen storage, it is favorable to intercept large wind amplitudes with a large wind farm, electrolyzer, and hydrogen storage. For no hydrogen storage, it is instead needed to stay feasible and meet the hydrogen demand.

The resulting storage capacities vary for both hydrogen storage and battery depending on the specific investment cost of hydrogen storage. This is illustrated in Figure 4.10b. Note that hydrogen storage capacity is given on the left y-axis in the unit GWh and battery storage capacity is given on the right y-axis in the unit MWh with a logarithmic scale. With a specific investment cost of 1,900 EUR/MWh for hydrogen storage, the resulting hydrogen storage capacity is 56.7 GWh, a threefold capacity compared to the reference case. With a specific investment cost of 45,000 EUR/MWh for hydrogen storage, the resulting hydrogen storage capacity is 13.1 GWh, 6.5 % smaller compared to the reference case. With a specific investment cost of 11,000 EUR/MWh for hydrogen storage, or higher, it is beneficial to invest in batteries. In the reference case, a battery storage capacity of 2.3 MWh is yielded. With a specific investment cost of 45,000 EUR/MWh for hydrogen storage, the battery storage capacity is 93 MWh. With no hydrogen storage, the resulting battery capacity is 7,258 MWh.

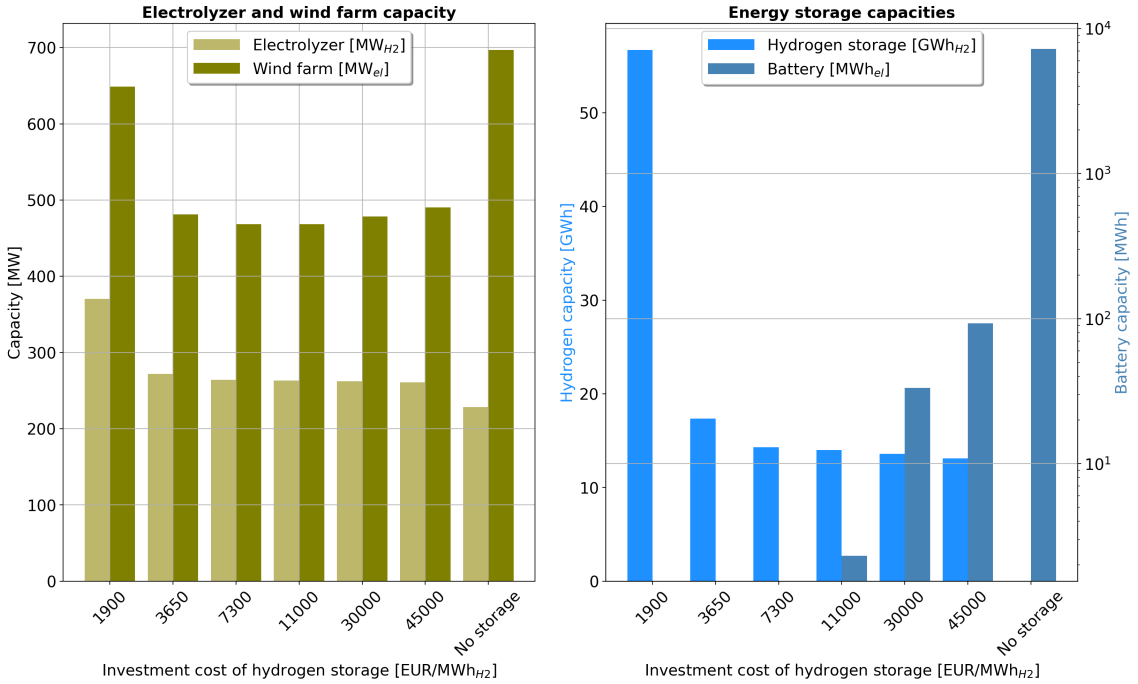

Figure 4.10: Resulting electrolyzer and wind farm capacity a). Resulting in energy storage capacity for different specific investment costs of hydrogen storage. Hydrogen storage capacity is given by the right y-axis measured in GWh and battery capacity is given by the right y-axis measured in MWh in a logarithmic scale b)

The SMR produces half, or more, of the hydrogen demand for all cases except for the cheapest specific investment cost of hydrogen storage of 1,900 EUR/MWh where the electrolyzer produces 55 % of the total hydrogen demand, shown in Figure 4.11. As earlier stated, this case has a larger electrolyzer, wind farm (Figure 4.10a), and hydrogen storage (Figure 4.10b) compared to the reference case, resulting in the lowest capacity factor (56.0 %) over the test range, shown in Figure 4.11. With no available hydrogen storage, the highest capacity factor (83.2 %) of the electrolyzer is obtained, see Figure 4.11. For the same case, the smallest electrolyzer capacity (228 MW$_{H2}$) is obtained.

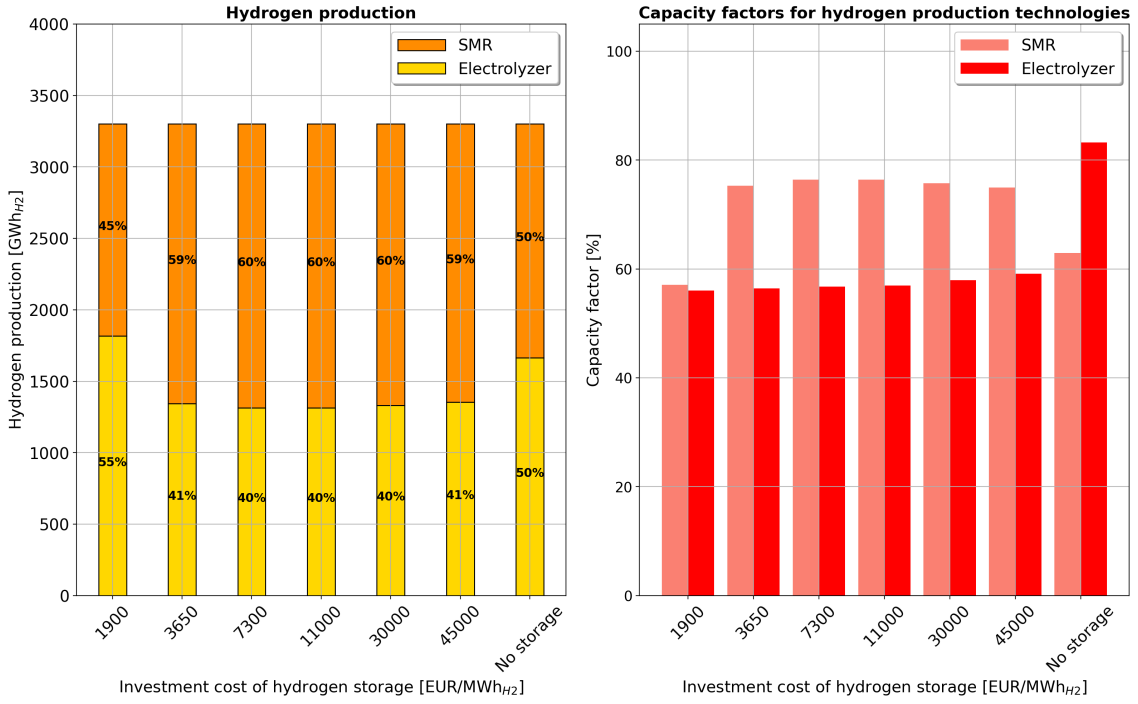

Figure 4.11: The annual hydrogen production from the hydrogen production technologies (SMR and electrolyzer)(a), and capacity factors for each hydrogen production technology (b).

4.2.3 Transmission capacity and forecasted spot prices

In this section, the results for varying the available transmission capacity between the refinery and the regional grid are presented. In the reference case, a transmission capacity of 15 MW and spot prices from 2019 were used. In addition, forecasted electricity spot prices for the year 2050 have been included in the analysis to analyze the impact of transmission capacity with a larger share of VRE in the electricity mix. The forecasted electricity prices for 2050 are described in Section 3.5.3. The overall impact of different transmission capacities regarding total system cost and LCOH is small and those results are therefore excluded from this section. In Appendix C, total system cost and LCOH with transmission capacities in the range of 0-60 MW are presented with spot prices from 2019 and forecasted spot prices for 2050.

In Figure 4.12a, electrolyzer and wind farm capacities are shown for different transmission capacities. Similar trends for the electrolyzer capacity with 2019 and 2050 spot prices are observed. For both cases, the electrolyzer capacity decreases as a larger transmission capacity between the grid and refinery is available. The larger share of VRE in the 2050 case have therefore a marginal effect on the electrolyzer capacity. However, the trends for wind farm capacity with spot prices from 2019 and 2050 differ. After 30 MW of transmission capacity, the resulting wind farm capacity starts to diverge for the different spot price datasets. With a transmission capacity of 60 MW, the wind farm capacity is 500 MW for 2019, compared to 461 MW for the year 2050. The energy storage capacities are presented for different transmission capacities in Figure 4.12b. The hydrogen storage capacity decreases from 17.5 GWh to 11.3 GWh when the transmission capacity is varied between 0-60 MW with 2019 spot prices. A similar reduction in hydrogen storage capacity is seen with spot prices for 2050, where the storage capacity decreases from 17.5 GWh to 12.5 GWh for the same range of transmission capacity. The overall trend is that the model favors slightly larger hydrogen storage with 2050 spot prices for larger transmission capacities. The battery storage capacity with spot prices for 2050 increases approximately linearly (0-4.8 MWh) with increasing transmission capacity (0-60 MW).

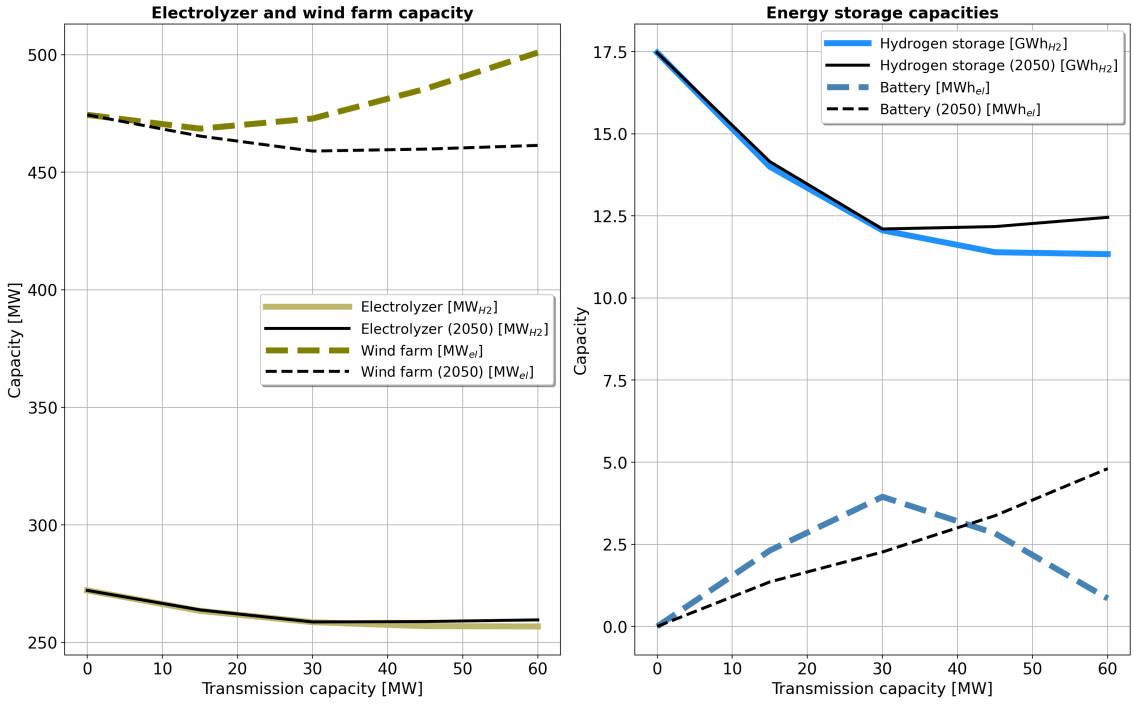

Figure 4.12: Electrolyzer and wind farm capacity for varying transmission capacities (a). Energy storage capacities with different available transmission capacities (b). Hydrogen storage capacity is given in GWh and battery storage capacity in MWh.

One question that arises from the presented trends is - why do the capacities in the electrolyzer, wind farm, and hydrogen storage stagnate for a transmission capacity larger than 30 MW for the 2050 spot price data meanwhile batteries increase? The answer will also explain why a larger wind farm is cost-beneficial for 2019 spot price data. The main contributing factor is the larger share of wind power in the electricity mix in 2050, compared to 2019 (Figure 3.2). In Figure 4.13, the spot price and wind profile correlation is presented. The figure shows the sorted weekly averaged wind profile in ascending order, and weekly averaged spot prices with the same indexation as the sorted wind profile. The figure shows that generally during high wind output (to the right in Figure 4.13) when there is a potential to export excess offshore wind electricity, the spot prices for 2050 are lower compared to 2019, and during low wind output (to the left in Figure 4.13) the spot prices are higher than during 2019. This means that it is more profitable to import and export electricity with spot prices from 2019 compared to 2050, and the benefit from a larger wind farm capacity then ceases, and the electrolyzer, and hydrogen storage follows the same trend as a consequence.

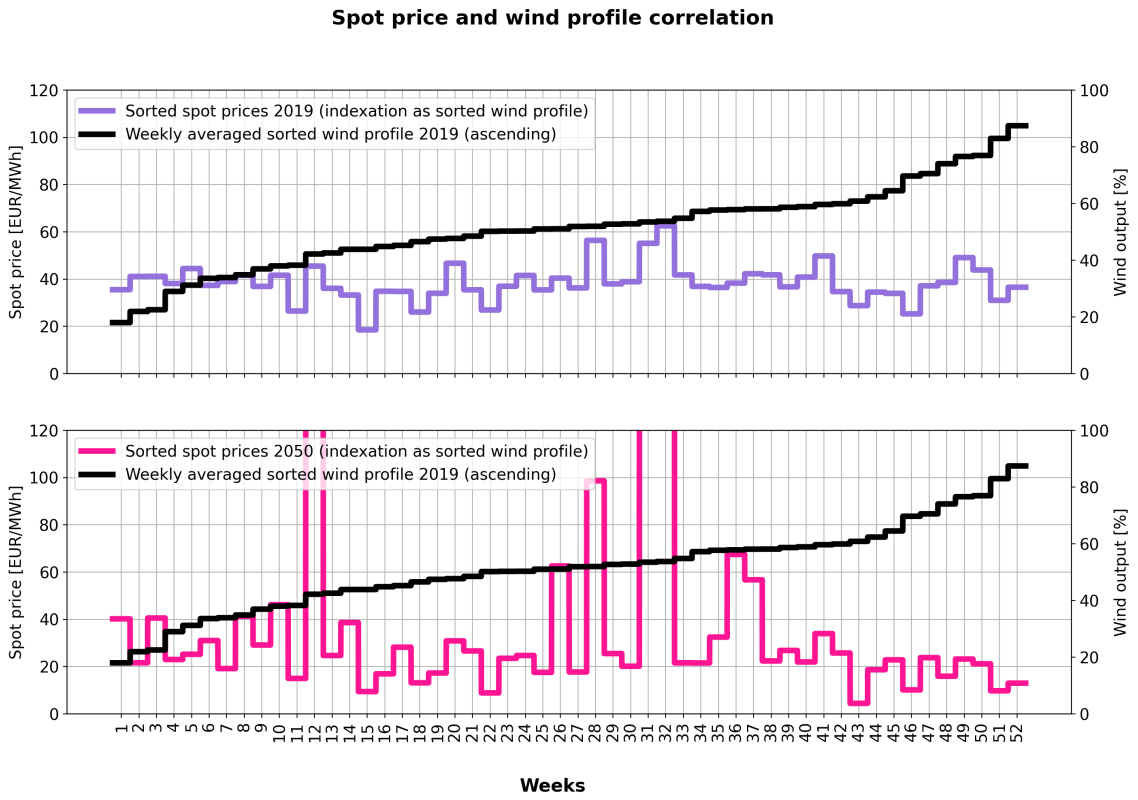

Figure 4.13: Wind profile and spot price correlation for spot prices from 2019 and forecasted spot prices for 2050. The wind profile is sorted and plotted by weekly average, and the spot prices are plotted with the same indexation as the sorted wind profile. The forecasted spot prices for 2050 are generated using input data from 2019. Note that the spot price peaks for 2050 are not seen in the figure (week 12 and weeks 31-32).

The results are reinforced by the trends seen in electricity import, export, and curtailment presented for different transmission capacities in the range of 0-60 MW in Figure 4.14a. The observed trend is that the model favors export rather than import with increasing transmission capacities, both with spot prices from 2019 and forecasted spot prices for 2050. The main observed difference between 2019 and 2050 spot prices is that the export is larger in the range of 30-60 MW of transmission capacity for the 2019 case, where the export increases from 44 GWh to 106 GWh. In the same range of transmission capacity, the export increases from 44 GWh to 67 GWh with forecasted spot prices for 2050. Curtailment decreases with increasing transmission capacity for both 2019 and 2050, and in the range of 30-60 MW of transmission capacity, the curtailment is 0 GWh. The trends for import and export are in line with the trend shown in Figure 4.13, where it is more profitable to import and export electricity with spot prices from 2019 compared to 2050.

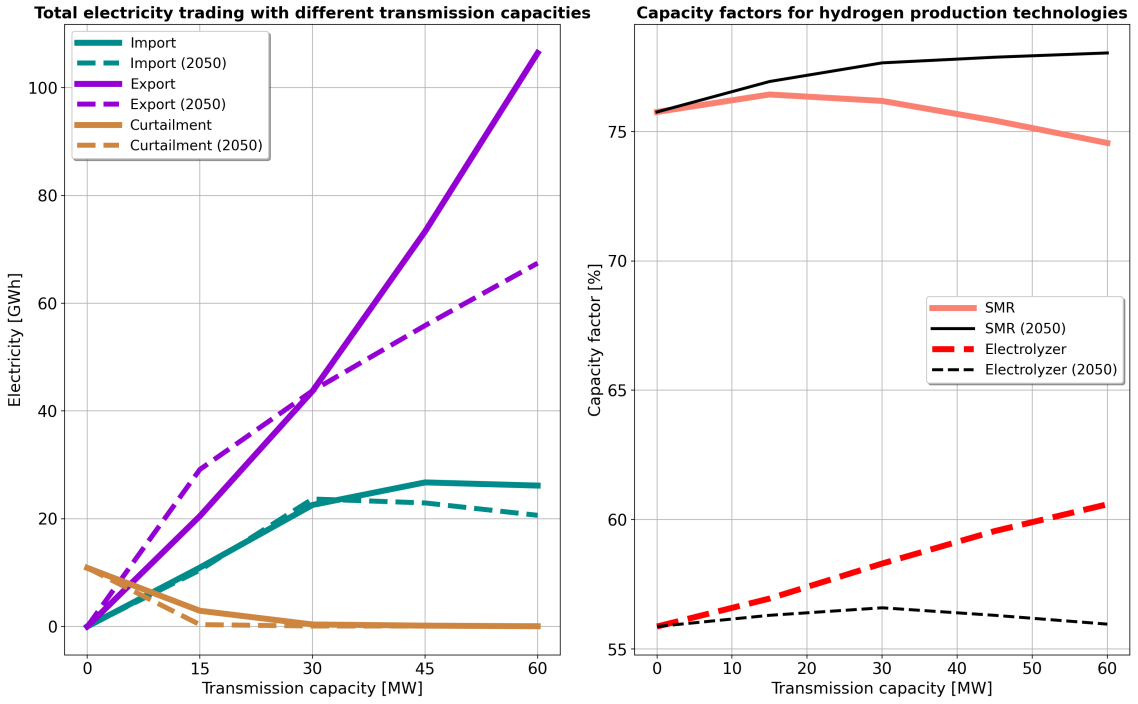

Figure 4.14: Electricity import, export, and curtailment for transmission capacities in the range 0-60 MW, with spot prices from 2019 and 2050 forecasted spot prices (a). Capacity factors for SMR and electrolyzer with transmission capacities in the range of 0-60 MW, with spot prices from 2019 and 2050 forecasted spot prices (b). Note that the y-axis does not start at 0.

The spot prices for 2050 are influenced by solar variations through imports from Europe (Figure 3.2), which explains why the model favors larger battery capacity with increasing transmission capacity. As stated in Section 2.1.1, batteries are proven to be suited for diurnal variations, such as solar variations. The trend for the battery capacity with spot prices from 2019 is different compared to 2050 (Figure 4.12). The battery capacity increases in the range of 0-30 MW of transmission capacity, where a maximum battery capacity is obtained of 3.95 MWh (30 MW transmission capacity) and decreases in the range of 30-60 MW of transmission capacity. The reduction in battery capacity in the range of 30-60 MW of transmission capacity corresponds with the increase in wind farm capacity in the same range of transmission capacity. Under these circumstances larger wind variations introduced by larger wind farm capacity results in less battery capacity. As stated in Section 2.1.1, batteries are proven to not be economically suited to manage large wind variations.

Capacity factors for the energy storages are presented for different transmission capacities in Figure 4.14b. The capacity factor for the SMR decreases from 75.8% to 74.6 % with 2019 spot prices in the range of 0-60 MW of transmission capacity. For the same range of transmission capacity, the SMR capacity factor increases from 76.9% to 78.0% with forecasted spot prices for 2050. Larger wind farm capacity (Figure 4.12a) for the year 2019 results in a lower capacity factor for the SMR, compared to 2050. Similar reasoning applies to the SMR capacity for the year 2050, where smaller wind farm capacity yields larger hydrogen production from the electrolyzer compared to 2019, which yields a lower capacity factor of the SMR for 2050 in relation to the year 2019. The electrolyzer capacity factor increases linearly from 55.9% to 60.6% in the range of 0-60 MW of transmission capacity with 2019 spot prices. The increase in capacity factor relates to the increase in wind farm capacity seen in Figure 4.12a. With spot prices for 2050, the resulting electrolyzer capacity is rather constant for different transmission capacities, where a small increase from 55.9% to 56.0 % is seen in the range 0-30 MW of transmission capacity and a small decrease from 56.0% to 55.9% in the range 30-60 MW.

4.2.4 Operational cost of the SMR

For all operational costs of the SMR in the range of 55-165 EUR/MWh, it is beneficial to invest in CCS capacity to cover 90 % of the CO_2 emissions emitted from the SMR. This means that the CCS capacity does not limit the operation of the SMR. In Figure 4.15a, one can see the total system cost, and in Figure 4.15b the LCOH for the green and blue systems are presented for different values of C^{op}_{smr}. With great uncertainties for each individual parameter for the variable cost, it is presented only as a total in this sensitivity analysis. Both the total system cost and LCOH_{blue} behave nearly proportionally with the operational cost of the SMR C^{op}_{smr} with no further investments in SMR capacity allowed. The levelized cost for the green system follows a different trend. There are two interesting observations for the levelized cost of hydrogen for the green system. The first observation is that LCOH_{green} is 19% higher with an operating cost of 55 EUR/MWh, compared to the reference case's LCOH_{green}. The second interesting observation is that the levelized cost of the green system increases by 9% when the operational cost is varied between 137-165 EUR/MWh. To explain these observations, the resulting capacities for different technologies and the hydrogen supply have to be presented.

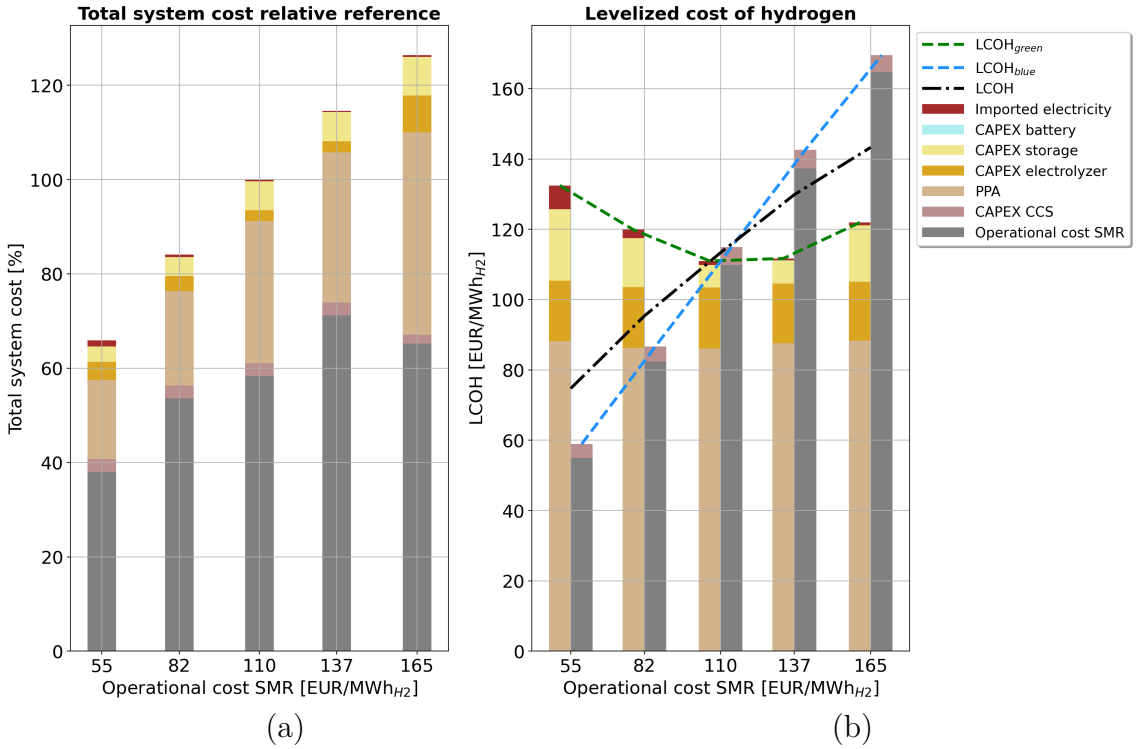

Figure 4.15: Total system cost relative to the reference case (110 EUR/MWh$_{H2}$) for operational costs in the range 55-165 EUR/MWh$_{H2}$ (a). Levelized cost of hydrogen for operational costs in the same range (b).

In Figure 4.16a, the resulting capacities of the electrolyzer and wind farm are presented. Both technologies follow the same trend, with increasing capacity for increased operational costs of the SMR C^{op}_{smr}. With an operational cost of 55 EUR/MWh$_{H2}$, investments in electrolyzer and wind farm are suppressed, resulting in 140 MW$_{H2}$ and 260 MW, seen in Figure 4.16a. Both capacities are approximately 45 % smaller compared to the reference case. In Figure 4.16b, the resulting energy storage capacities are shown. Both a lower and higher C^{op}_{smr} compared to the reference value of 110 EUR/MWh$_{H2}$ yields a larger hydrogen storage capacity. For the lowest operational cost in the test range (55 EUR/MWh), the resulting hydrogen storage capacity is 24.0 GWh, which is 71.0 % larger compared to the reference case. For the highest operational cost in the test range (165 EUR/MWh), the resulting hydrogen storage capacity is 48.7 GWh, which is 3.5 times the reference capacity.

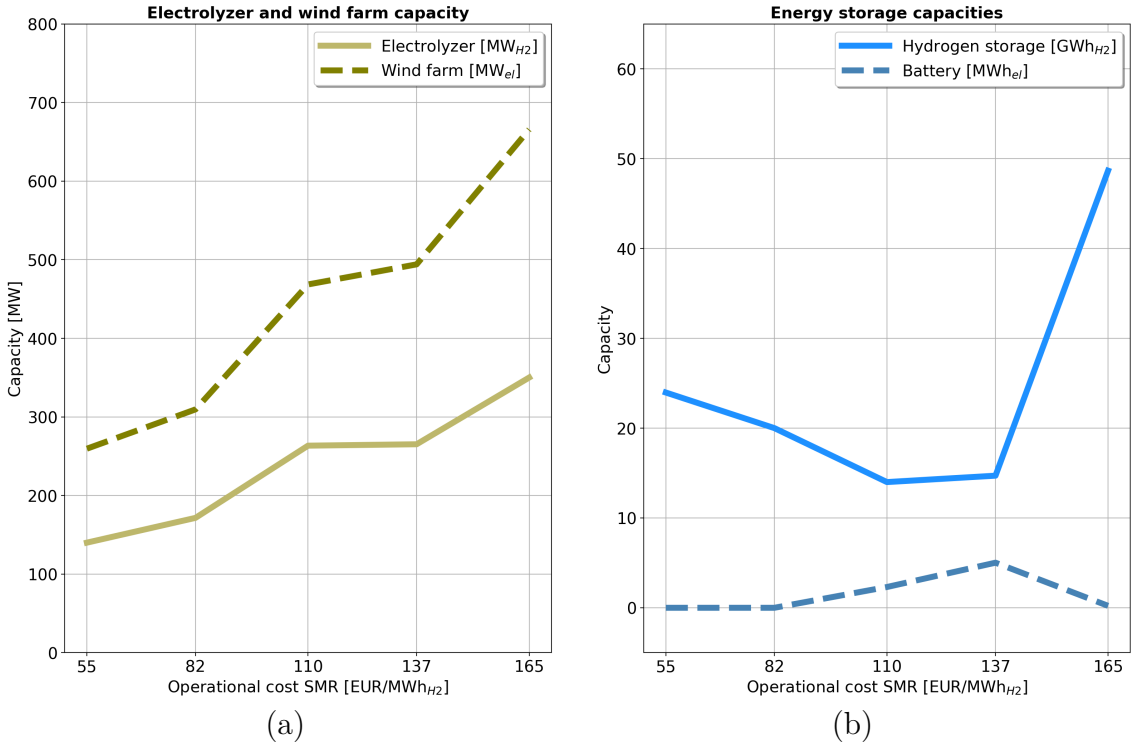

Figure 4.16: Capacities for (a) electrolyzer and wind farm and (b) energy storages.

The relatively large hydrogen storage capacity for the case with an operational cost of 55 EUR/MWh is a contributing factor for the high levelized cost of hydrogen for the green system, compared to the reference case. Due to the low operational cost of the SMR, it is operated at full capacity, which can be seen in Figure 4.17a. With no further investment in SMR capacity allowed, means that the electrolyzer and hydrogen storage supply the remaining parts of the hydrogen demand. Between hours 4,500-5,300 the dimensioning time period for the hydrogen storage occurs (Figure 4.17b), where the storage is fully discharged. Due to the system configuration, with a relatively small electrolyzer and wind farm capacity, an over-investment in hydrogen storage capacity is needed to meet the demand during the dimensioning time period. When the SMR is operated at full capacity over the year, in combination with an over-investment in hydrogen storage capacity, the storage is poorly utilized. This causes a higher levelized cost for the green system compared to the reference case.

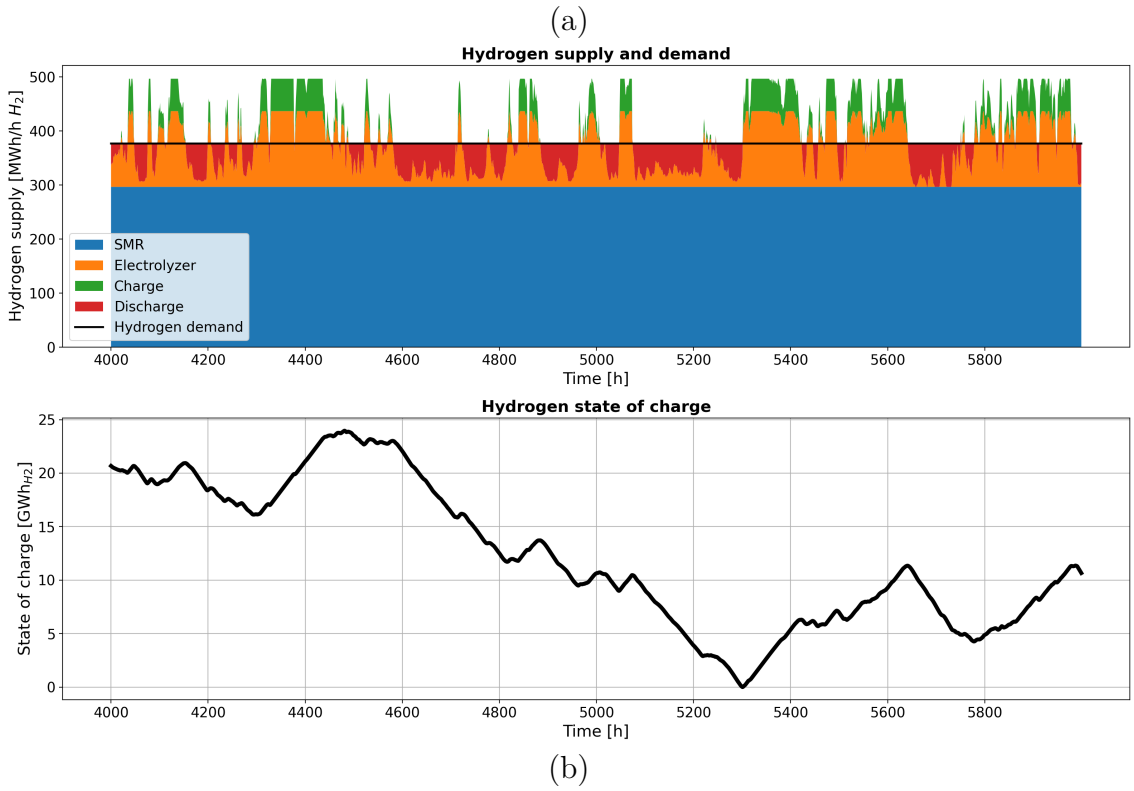

Figure 4.17: Hydrogen supply (a) and state of charge (b) for 2,000 hours when the dimensioning time period occurs. OPEX set to 55 EUR/MWh$_{H2}$.

The second interesting observation regarding the levelized cost of the green system is that the green hydrogen system composition changes significantly when C_{smr}^{op} is changed from 137 to 165 EUR/MWh$_{H2}$. In Figure 4.18a-c, the hydrogen supply is presented for operational costs in the range of 110-165 EUR/MWh for arbitrary 1,500 hours. The operational pattern for the SMR for the cases where the operational cost is 110 EUR/MWh and 137 EUR/MWh is similar. The SMR is operated on a high load when the hydrogen storage is discharged, which corresponds to periods with low wind output from the wind farm. The SMR is therefore managing wind variations. However, in Figure 4.18c, it is no longer cost-beneficial to manage wind variations with the SMR. The operational cost of the SMR is high enough to yield a larger capacity of the wind farm, electrolyzer, and storage capacity (Figure 4.16a-b). These investments result in a 9 % higher levelized cost for the green system with an operational cost of 165 EUR/MWh, compared to the reference case (110 EUR/MWh).

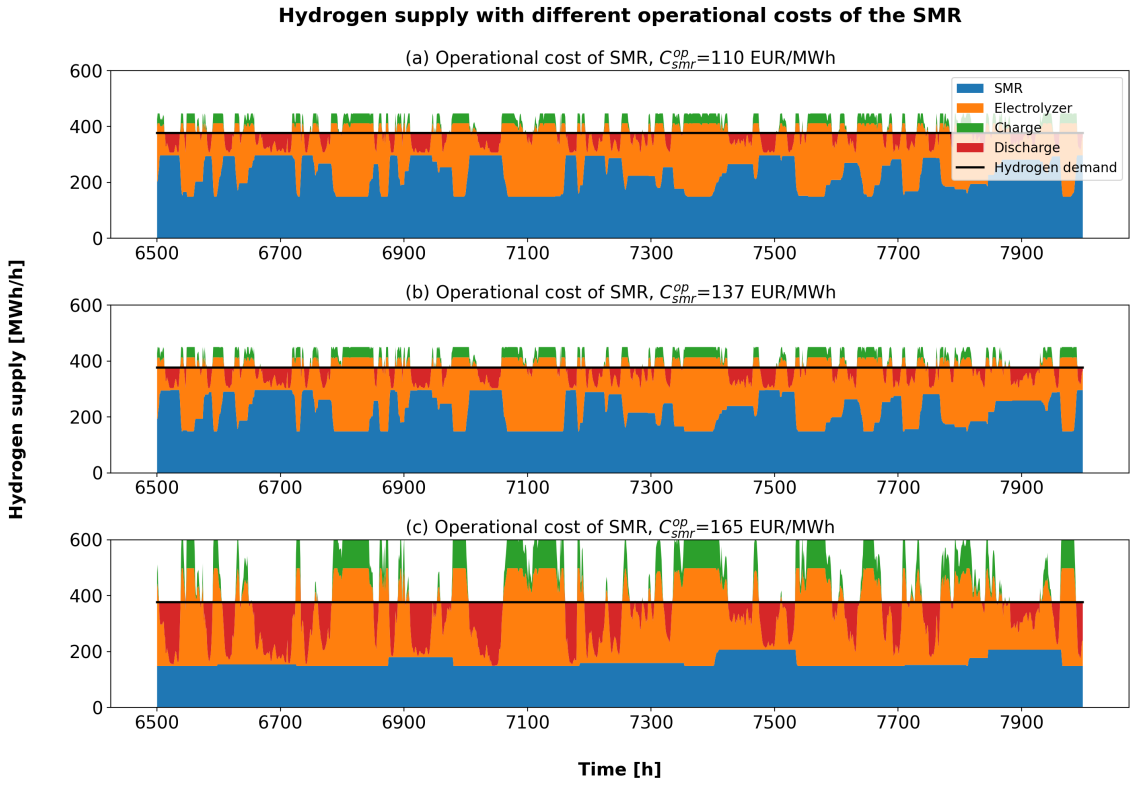

Figure 4.18: Hydrogen supply with different operational costs for the SMR. In (a) and (b), the operational cost is set to 110 EUR/MWh and 137 EUR/MWh, respectively. The load of the SMR increases when the storage is discharged. With an operating cost of 165 EUR/MWh, seen in (c), the SMR is mainly operated on minimum load and does not increase in load during hydrogen storage discharge.

Figure 4.19 shows that the increased operational cost of the SMR yields more curtailment. With the increasing operational cost of the SMR, the wind farm capacity increases as well (Figure 4.16a). This results in an increase of curtailment from 2.9 GWh to 73.6 GWh over the test range 110-165 EUR/MWh$_{H2}$. An increasing wind farm capacity suppresses the need for the import of electricity and the limited transmission capacity limits the export when curtailment occurs.

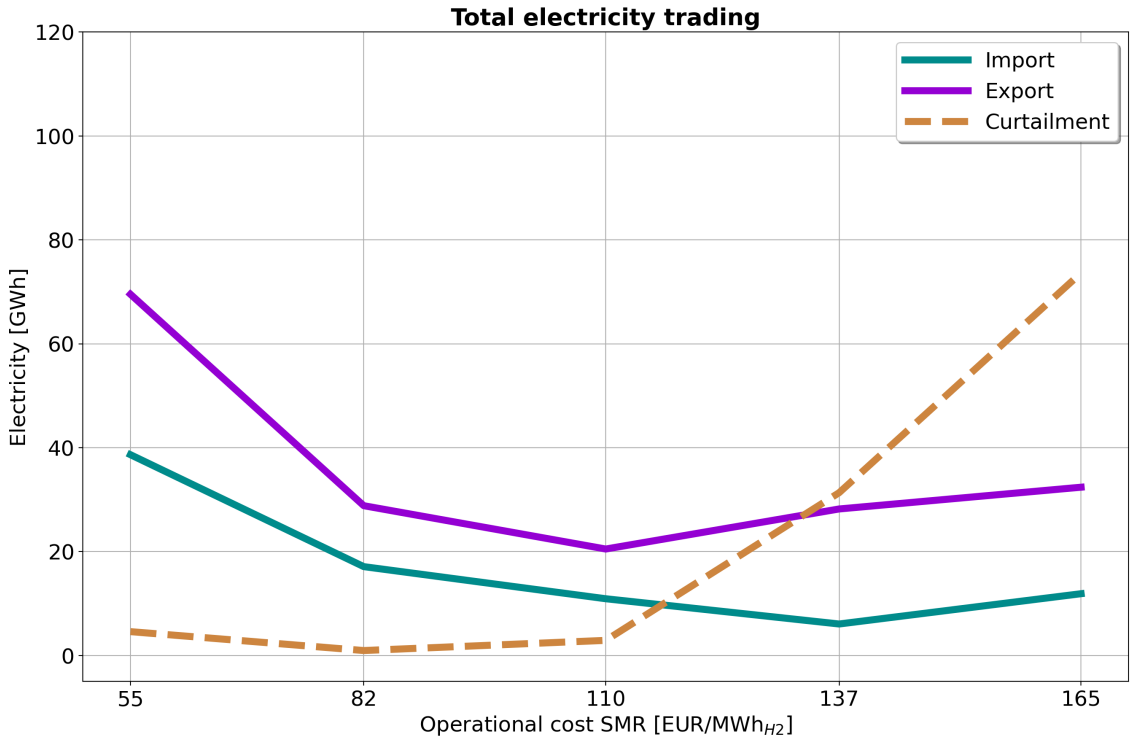

Figure 4.19: Export and import are suppressed with increased OPEX of the SMR, meanwhile curtailment increases.

With increasing OPEX for the SMR, its capacity factor declines, from 99.7 % to 57.0 % over the test range, see Figure 4.20a. The electrolyzer is subjected to the wind profile and transmission capacity and has an average capacity factor of approximately 57 % over the test range, see Figure 4.20b.

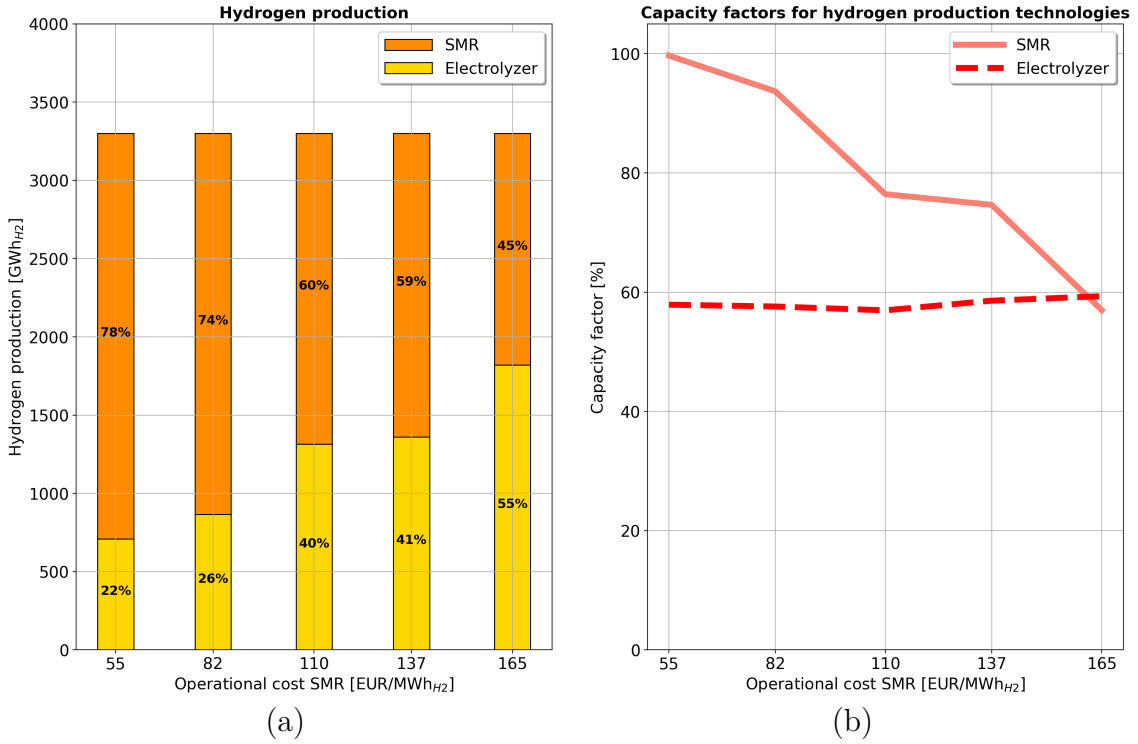

(a) (b)

Figure 4.20: Hydrogen production (a) and capacity factors (b) for the SMR and electrolyzer with operational costs of the SMR in the range 55-165 EUR/MWh.

4.2.5 Wind profiles

The sensitivity analysis of the GIS wind profiles is carried out in two steps. Firstly, the different GIS profiles are investigated isolated from each other, to see how each profile affects the system. Secondly, a consecutive model run is conducted, to see if the system is sensitive to annual weather variations.

Isolated model runs

The results of the optimization model do overall show small changes in hydrogen storage, electrolyzer, and wind farm capacity for different GIS wind profiles when run isolated from each other, shown in Table 4.2. GIS wind profile 2018 has the lowest capacity factor of 49.1 %, Equation (3.32), the smallest battery capacity of the five investigated wind profiles, the largest capacities in hydrogen storage, electrolyzer, and wind farm, and the highest total system cost (377 MEUR/yr). GIS wind profile 2015 has the highest capacity factor (58.0 %), the largest battery capacity, the smallest resulting wind farm capacity and total system cost (370 MEUR/yr), and the second smallest hydrogen storage capacity.

Table 4.2: Capacity factor and resulting hydrogen storage, electrolyzer, and wind farm capacity. GIS 2019 is the reference case.

Profile	Capacity factor, [%]	Total system cost, [MEUR/yr]	Hydrogen storage, [GWh]	Battery, [MWh]	Electrolyzer, [MW]	Wind farm, [MW]
GIS 2015	58.0	370	13.81	15.5	263	455
GIS 2016	51.4	374	13.89	4.9	263	466
GIS 2017	55.1	371	13.71	12.9	263	463
GIS 2018	49.1	377	16.26	0.33	269	484
GIS 2019	51.4	374	14.00	2.31	263	469

Figure 4.21 and 4.22 shows the GIS wind profiles of the years 2015 and 2018 and their respective

monthly and yearly wind profile average. For both profiles, the monthly average is consecutively under the yearly average for their dimensioning time period. For GIS wind profile 2015, the dimensioning time period can be found between the latter part of May and the beginning of November, where the monthly average is consecutively under the yearly average. For GIS wind profile 2018, it is found between the latter part of April and the latter of September.

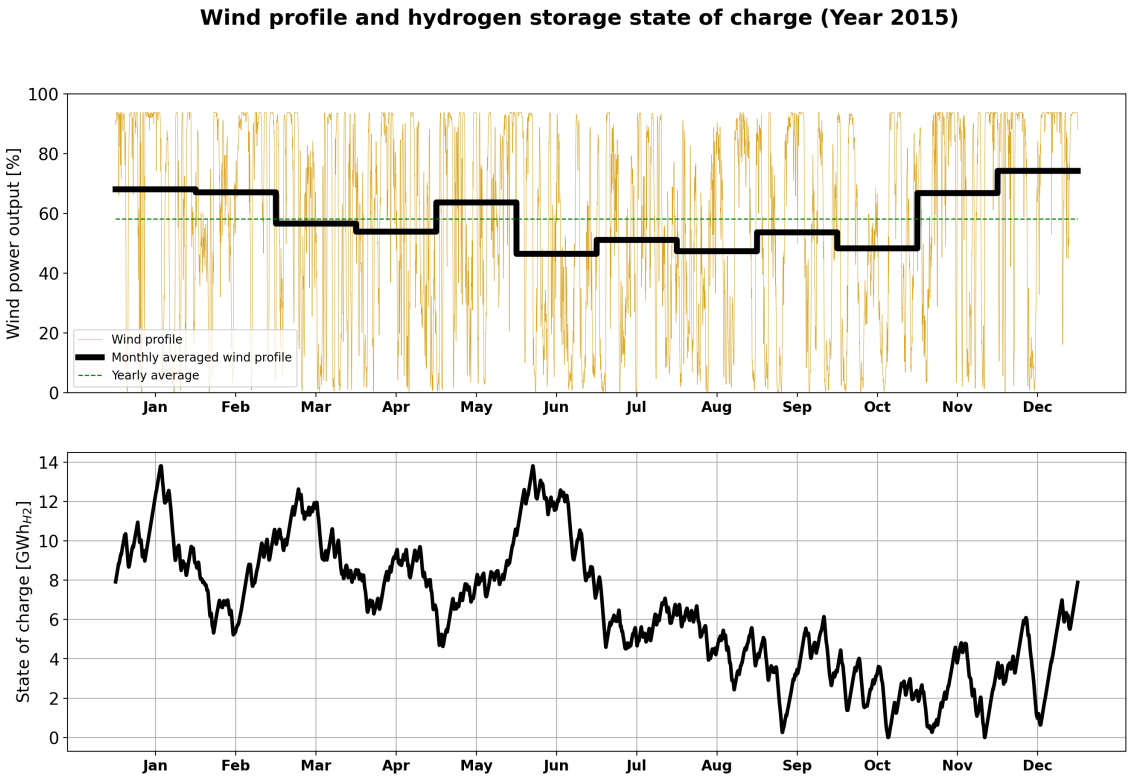

Figure 4.21: Normalized wind profile and monthly, and yearly wind profile average for 2015.

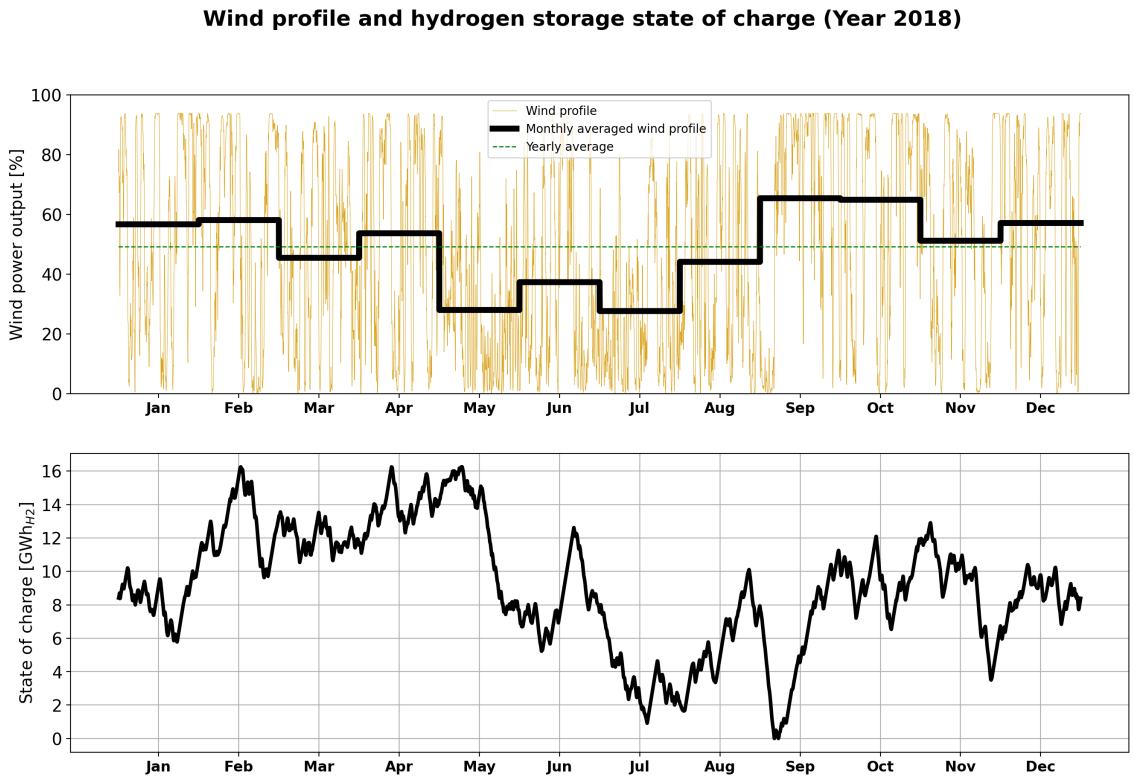

Figure 4.22: Normalized wind profile and monthly, and yearly wind profile average for 2018.

Consecutive model run

The consecutive model run is conducted over the years 2015-2019 by associating GIS wind profile and electricity spot price. Table 4.3 shows the resulting annual total system cost, capacities of energy storage, electrolyzer, and wind farm capacities. The consecutive model run results in an annual total system cost of 379 million euros, being 1.3 % more expensive compared to the reference case. The capacities obtained for hydrogen storage, electrolyzer, and wind farm are approximately the same as in the model run with GIS 2018 wind profile. Investing in batteries was beneficial for all GIS wind profiles (Table 4.2), but the consecutive model run results in zero battery capacity. In the consecutive model run the electrolyzer and hydrogen storage are dimensioned by the "dimensioning time period" for the year with the lowest wind profile capacity factor (2018). In relation to the remaining years in the consecutive model run, the electrolyzer and hydrogen storage are over-dimensioned, which might explain why the battery is not included in the cost-optimal technology composition for the consecutive model run.

Table 4.3: Resulting energy storage, electrolyzer, and wind farm capacities.

Case	Total system cost, [MEUR/yr]	Hydrogen storage, [GWh]	Battery, [MWh]	Electrolyzer capacity, [MW$_{H2}$]	Wind farm capacity, [MW]
Consecutive model run	379	16.26	0	269	475
GIS 2018	377	16.26	0.33	269	484
Reference case	374	14.00	2.31	263	469

Table 4.4 shows the annual import, export, and curtailment in the system. In 2018, 28.0 GWh of electricity was imported from the grid, and in 2015, 26.7 GWh was exported to the grid.

Table 4.4: Import, export, and curtailment during each year in the consecutive model run.

Profile	Import, [GWh]	Export, [GWh]	Curtailment, [GWh]
GIS 2015	0.046	26.7	0.69
GIS 2016	0	17.9	0.38
GIS 2017	0.015	23.2	0.55
GIS 2018	28.0	18.8	0.77
GIS 2019	2.90	18.5	3.44

In Figure 4.23 the SOC of the hydrogen storage is shown. In total, the storage is cycled five times (time between fully charged, discharged, and charged again), one time each year.

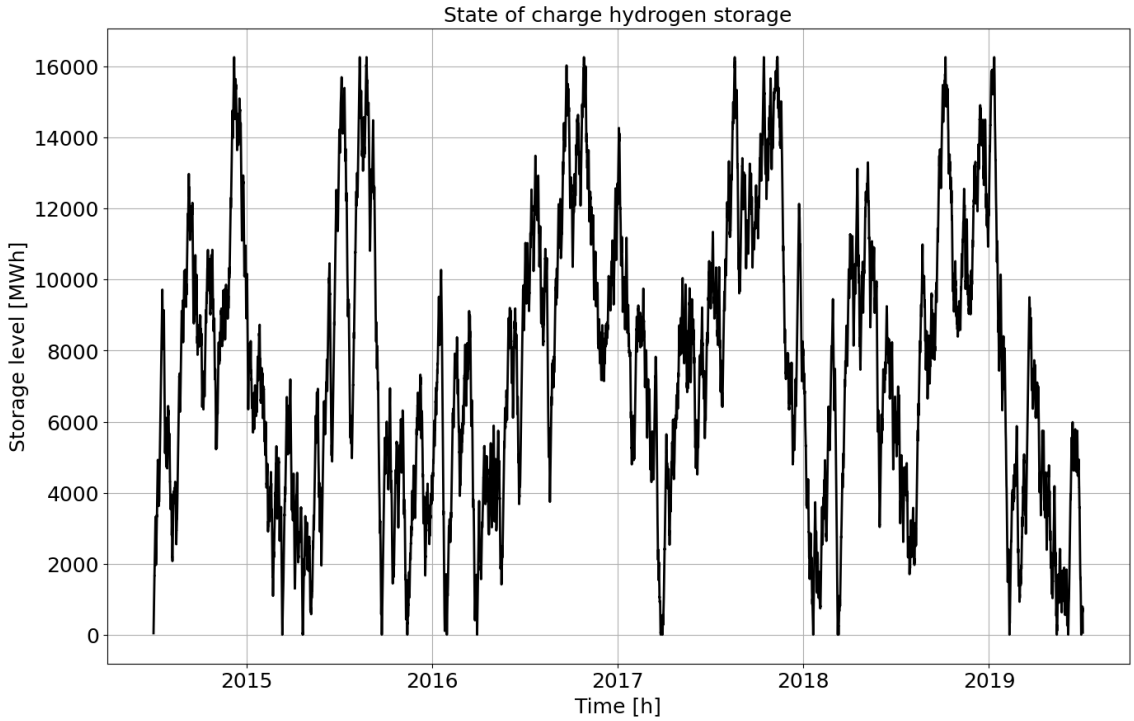

Figure 4.23: Five cycles, one for each year, are measured over the simulated period.

5
Discussion

In this thesis, the interaction between a green and a blue hydrogen system for a net zero refinery has been studied. The refinery hydrogen system has been studied standalone, which means that other processes at the refinery have not been included in the analysis. All carbon emissions related to the operation of the SMR are therefore accounted for through the EU ETS. In reality, fossil carbon dioxide emissions from the SMR can be compensated by negative emissions from other processes at the refinery (BECCS), or by employing CCS in combination with biogenic off-gases (BECCS).

The results in this thesis should not be seen as investment and portfolio research, but rather as an analysis of how the different technologies interact with each other under certain circumstances, and an approximation of the required dimensions of the green hydrogen system to meet the refinery hydrogen demand with fixed capacity of the SMR. In the sensitivity analysis, one model parameter was varied at a time. The effects of changing multiple parameters simultaneously are not considered in this thesis, but such scenario-based analysis could potentially yield further information on the interaction between the blue and green hydrogen systems.

The developed linear cost-optimization model used in this thesis is time-efficient to run and yields both cost-optimal technology capacities and dispatch patterns of technologies for the given circumstances. Even with a model run for five consecutive years with an hourly resolution, the model is solved within minutes in GAMS. Introducing binary variables has been avoided since it severely increases the computational time and could potentially compromise the cost-optimality of the model. Though to enable analyzing the impacts of revisions to the system or the impact of completely shutting down certain technologies, one would have to extend the model to a mixed-integer programming model.

The energy-only model uses an hourly resolution to intercept variability in wind, spot prices, and the ramping constraints of the SMR. With the assumptions of a pay-as-produced PPA and available grid connection, the electrolyzer manages to follow the wind profile to a large extent and obtains a higher capacity factor than the wind profile itself meanwhile mitigating curtailment. The PPA can yield energy security and be a strategy to account for more volatile spot prices in the future. As the results show, the system is affected by wind-dominated spot prices of the year 2050, where the benefit of electricity trading is less substantial compared to the year 2019. On the other hand, the cannibalization effect diminishes the flexibility of transmission capacity when the electricity spot price is wind-dominated. For the highest tested operational cost of the SMR (165 EUR/MWh$_{H2}$), it is not cost-efficient to manage wind variations with the SMR. In the intermediate cost range (82-137 EUR/MWh$_{H2}$), with the prevailing assumptions, the SMR manages wind variations and mitigates overcapacity in the green hydrogen system.

With all parameters known beforehand, the model has perfect foresight. The concept of perfect foresight and wind variability is investigated with different wind profiles in a consecutive model run, which yields approximately the same system composition and total system cost as the model runs with isolated wind profiles. However, the simulations conducted with isolated wind profiles show that investments in batteries would be the optimal system composition, but in the consecutive model run investments in batteries are suppressed. A definite conclusion regarding the battery capacity can not be drawn from the presented results in this study. However, in model runs where

battery capacity is included in the cost-optimal technology composition, the battery is used for mitigating curtailment and increasing the capacity factor of the electrolyzer. The results also show that batteries become more competitive with more volatile spot prices (2050) in combination with larger transmission capacity (60 MW).

Depending on the specific investment cost for hydrogen storage, the resulting capacity for electrolyzer and wind farm is insensitive in the span of 3,650-45,000 EUR/MWh. The specific investment cost for LRC is uncertain and a high specific cost is used compared to what can be found in the literature. With high specific investment costs (30,000-45,000 EUR/MWh) batteries become more competitive than before compared to hydrogen storage. In the case where hydrogen storage is disabled, a battery capacity of 7,258 MWh is obtained. This is an unreasonable size considering the sizes currently being deployed in Sweden and its inability to store electricity over seasonal periods. With batteries being subjected to a more detailed description of current leakage, the hydrogen production system would become more expensive, or even unfeasible, to operate with a pay-as-produce PPA without any hydrogen storage.

The majority of the expenses regarding the total system cost relate to the OPEX of the hydrogen system. The operational cost of the SMR and the electricity bought via PPA account for 88.5% of the total system cost for the reference case. The operational costs of the SMR (Equation (3.22)) consist of three parameters, where two are decided and varying with existing markets (EU ETS and price of natural gas). In reality, the operational expenses for the SMR would be fluctuating with the price of natural gas and EU ETS and not be static as modulated in the cost optimization model. This would result in periods with relatively low and high operational expenses for the SMR over the year. With low OPEX for the SMR, the green hydrogen system becomes poorly utilized, and with high OPEX, the minimum load of the SMR becomes the binding model constraint. The minimum load stems from the need to combust and utilize excess off-gases from refining processes. With the possibility to store excess off-gases, it could be possible to ramp down the SMR during high-cost scenarios, but with no insight into the possibility from a refining perspective, this is left to future research. With a pay-as-produce PPA, one will be forced to utilize the received electricity, no matter the operational cost of the SMR. On the other hand, with a baseload PPA, the scenario would be similar. One would still be subjected to buy a certain amount of electricity on average to fulfill the power purchase agreement.

6
Conclusion

The interplay between a blue hydrogen system consisting of a steam methane reformer (SMR) with employed carbon capture and storage (CCS), and a green hydrogen system consisting of an electrolyzer, hydrogen storage, battery storage, and offshore wind farm with a pay-as-produced power purchase agreement (PPA) is assessed for a net zero refinery using a techno-economic cost-optimization model. The model shows that existing fossil-based hydrogen production can be partly replaced by a new green hydrogen system, operated in parallel with a blue hydrogen system with a 90 % capture rate CCS that meets a continuous hydrogen demand of 377 MW. The resulting levelized cost of hydrogen is 111 EUR/MWh for the green hydrogen system and 115 EUR/MWh for the blue system. The green system comprises a 263 MW_{H2} electrolyzer, 469 MW offshore wind farm, 14 GWh hydrogen storage, and 2.3 MWh battery.

A number of flexibility measures have been identified in this thesis. The electrolyzer manages to follow the wind profile, with excess hydrogen production the hydrogen storage is charged, and with low wind power output the storage is discharged. To mitigate curtailment, the battery is charged and later discharged to either supply electricity to the electrolyzer or export to the regional grid. Transmission capacity mitigates overinvestment in the green hydrogen system. With electricity spot price data, depending on a European electricity mix with a 64 % wind power share (2050), the system suffers from the cannibalization effect with a transmission capacity of 30 MW or larger. Wind variability over different years is tested and results show it has a small impact on the system composition but with a consecutive model run over five years, the model is subjected to the year with the lowest capacity factor.

Based on results from sensitivity analysis it is found that hydrogen storage is crucial for mitigating total system cost with a pay-as-produced PPA. The cost-optimization model and its system composition are sensitive to the operational expenses of the SMR, which constitute of the cost of CCS with a 90 % capture rate, the cost of carbon dioxide emissions being leaked, and natural gas. For operational expenses of 82-137 EUR/MWh_{H2}, the SMR mitigates the effect of wind variations, resulting in fewer over-investments in the green hydrogen system.

Bibliography

[1] E. Commission, "A European Green Deal," Accessed May 05, 2023. https://commission.europa.eu/strategy-and-policy/priorities-2019-2024/european-green-deal.

[2] G. Erbach and L. Jensen, "EU hydrogen policy - Hydrogen as an energy carrier for a climate-neutral economy," Accessed May 15, 2023. https://www.europarl.europa.eu/RegData/etudes/BRIE/2021/689332/EPRS-BRI(2021)689332-EN.pdf.

[3] IEA, "The Future of Hydrogen," June 2019. Accessed May 05, 2023. https://www.iea.org/reports/the-future-of-hydrogen.

[4] IEA, "Global Hydrogen Review 2022," Accessed May 05, 2023. https://iea.blob.core.windows.net/assets/c5bc75b1-9e4d-460d-9056-6e8e626a11c4/GlobalHydrogenReview2022.pdf.

[5] Preem, "We are bringing forward our climate target by ten years – from 2045 to 2035." Accessed Mar 10, 2023. www.preem.com/climate-target-2035/.

[6] Preem, "Europe's most modern refineries," Accessed May 20, 2023. https://www.preem.com/in-english/about/refineries/.

[7] A. Karre, "Basics of hydrotreating units," June 2020. Accessed Feb 28, 2023. https://www.worldofchemicals.com/media/basics-of-hydrotreating-units/4340.html.

[8] A. LaFleur, *Use and Optimization of Hydrogen at Oil Refineries*. Shell, May 2017. Accessed Feb 28, 2023. https://www.energy.gov/sites/prod/files.

[9] S. Hicks and P. Gross, "Hydrogen for refineries is increasingly provided by industrial suppliers," *U.S. Energy Information Administration*, January 2016. Accessed Feb 28, 2023. https://www.eia.gov/todayinenergy.

[10] M.Tagliabue, "Refinery off-gas in hydrogen production," April 2022. Accessed Apr 11, 2023. https://www.digitalrefining.com/article/1002727/refinery-off-gas-in-hydrogen-production.

[11] *Meeting refinery needs for hydrogen*. Linde Engineering. Accessed Feb 28, 2023. www.linde-engineering.com/en/about-linde-engineering/success-stories/h2-as-industrial-gas.html.

[12] J. G. Speight, "Industrial Utilization of Hydrogen," *Hydrogen Science and Engineering: Materials, Processes, Systems and Technology*, 2016. Accessed Feb 28, 2023. https://onlinelibrary.wiley.com/doi/pdf/10.1002/9783527674268.ch01.

[13] "Hydrogen Production: Natural Gas Reforming," Accessed Apr 11, 2023. https://www.energy.gov/eere/fuelcells/hydrogen-production-natural-gas-reforming.

[14] Z. Byrum and C. Dellesky, "A Low-Carbon Future in the US Depends on Decarbonizing Petroleum Refineries," October 2021. Accessed Apr 13, 2023. https://www.wri.org/insights/technologies-decarbonize-petroleum-refineries.

[15] IEA, "Biofuels," 2021. Accessed Apr 13, 2023. https://www.iea.org/reports/renewables-2021/biofuels.

[16] M. S. Lester, R. Bramstoft, and M. Münster, "Analysis on electrofuels in future energy systems: A 2050 case study," *Energy*, vol. 199, p. 117408, 2020.

[17] A.Schäfer, H.Schuster, U.Kasper, and A.Moser, *Electrochemical Energy Storage for Renewable Sources and Grid Balancing*. Elsevier, 2015.

[18] L.Göransson, "Balancing Electricity Supply and Demand in a Carbon-Neutral Northern Europe," *Energies*, 2023. Accessed May 22, 2023. https://doi.org/10.3390/en16083548.

[19] "Technology Data, Energy Storage, Hydrogen Storage," January 2020. Accessed Mar 22, 2023. www.ens.dk/sites/ens.dk/technology_data_catalogue_for_energy_storage.pdf.

[20] "Hydrogen Storage," *Hybrit*. Accessed Mar 22, 2023. https://www.hybritdevelopment.se/en/a-fossil-free-development/hydrogen-storage/.

[21] P.Tengborg, J.Johansson, and D.Durup, "Storage of highly compressed gases in underground Lined Rock Caverns – More than 10 years of experience," 2014. Accessed Mar 13, 2023. www.researchgate.net.

[22] O.Kruck, R.Prelicz, and T.Rudolph, "Overview on all Known Underground Storage Technologies for Hydrogen," *HyUnder*, August 2013. Accesed Mar 22, 2023. www.hyunder.eu/Overview-of-all-known-underground-storage-technologies.pdf.

[23] J.Andersson and S. Grönkvist, "A comparison of two hydrogen storages in a fossil-free direct reduced iron process," tech. rep., Division of Energy Processes, July 2018. Accesed Mar 22, 2023. https://reader.elsevier.com/reader.

[24] D.Papadias and R. Ahluwalia, "Bulk storage of hydrogen," *Argonne National Laboratory*, August 2021. Accesed Mar 22, 2023. www.anl.gov/argonne-scientific-publications/pub/164523.

[25] A.Toktarova, V.Walter, L.Goransson, and F.Johnsson, "Interaction between electrified steel production and the north european electricity system," *Applied Energy*, March 15, 2022. Accesed Feb 01, 2023. https://www.sciencedirect.com/science/article/pii/S0306261922000654?via%3Dihub.

[26] F.Johansson, J.Spross, D.Damasceno, J.Johansson, and H.Stille, "Investigation of research needs regarding the storage of hydrogen gas in lined rock caverns. (English) [Prestudy for Work Package 2.3 in HYBRIT Research Program 1]," tech. rep., School of Architecture and the Built Environment, Department of Civil and Architectural Engineering, Division of Soil and Rock Mechanics, 2018. Accesed Mar 22, 2023. http://kth.diva-portal.org/smash/get/diva2:1221714/FULLTEXT01.pdf.

[27] "Technology Data, Energy Storage, Lithium-ion batteries for grid-scale storage," *Danish Energy Agency*, January 2019. Accessed Mar 27, 2023. www.ens.dk/sites/ens.dk/technology_data_catalogue_for_energy_storage.pdf.

[28] V.Henze, "Lithium-ion Battery Pack Prices Rise for First Time to an Average of $151/kwh," *BloombergNEF*, December 6, 2022. Accesed Mar 27, 2023. https://about.bnef.com/blog/lithium-ion-battery-pack-prices-rise-for-first-time-to-an-average-of-151-kwh/.

[29] Axpo, "Axpo to build battery storage in Sweden," Accessed May 14, 2023. https://www.axpo.com/hr/en/about-us/media-and-politics/media-releases.detail.html/media-releases/2023/axpo-to-build-battery-storage-in-sweden.html.

[30] K. et al., "A review of battery energy storage systems for ancillary services in distribution grids: Current status, challenges and future directions," *Frontiers in Energy Research*, September 16 2022. Accessed May 14, 2023. https://www.frontiersin.org/articles/10.3389/fenrg.2022.971704/full.

[31] S. Kraftnät, "Bidra med reserver," Accessed May 14, 2023. https://www.svk.se/aktorsportalen/bidra-med-reserver/.

[32] C. de Jong, "PPA Insights: Renewable contract structures and valuation." Accessed Mar 1, 2023. www.kyos.com/ppa-insights-on-renewable-contract-structures-and-valuation/.

[33] C. Richard, "Sweden's developers offer Europe's "cheapest wind PPAs"," *Windpower Monthly*, October 2020. Accessed Feb 27, 2023. www.windpowermonthly.com/article/1697414/swedens-developers-offer-europes-cheapest-wind-ppas.

[34] "PPA - en nyckel i finansieringen av ny kraftproduktion," Accessed Mar 21, 2023. https://svenskvindenergi.org/wp-content/uploads/2021/05/PPA-ett-faktablad-fran-Svensk-Vindenergi.pdf.

[35] Å.Elmqvist, M. Wondollek, and M. Kofod-Hansen, *El från nya anläggningar (Swedish)*. 2021:714, Energiforsk, December 2021. Accessed Mar 1, 2023. energiforsk.se/media/30970/el-fra-n-nya-anla-ggningar-energiforskrapport-2021-714.pdf.

[36] K. Comstedt Webb, *Innovativt samarbete mellan OX2 och Cementa på Gotland (Swedish)*. Cementa, June 2022. Accessed Mar 1, 2023. www.cementa.se/sv/innovativt-samarbete-mellan-ox2-och-cementa-pa-gotland.

[37] Vattenfall, "Minska industrins koldioxidutsläpp, (Swdish)." Accessed Mar 1, 2023. www.vattenfall.com/se/var-verksamhet/vagen-mot-ett-fossilfritt-liv/minska-industrins-koldioxidutslapp/preem.

[38] Vattenfall, "Minska industrins koldioxidutsläpp, (Swdish)." Accessed Mar 1, 2023. www.vattenfall.com/se/var-verksamhet/vagen-mot-ett-fossilfritt-liv/minska-industrins-koldioxidutslapp/st1.

[39] M.Biermann et al., "Preem CCS Synthesis of main project findings and insights," February, 2022. Accessed Apr 20, 2023. https://research.chalmers.se/en/publication/528685.

[40] "EU Emissions Trading System (EU ETS)," *European Commission*. Accessed Apr 20, 2023. www.eu-emissions-trading-system-eu-ets.

[41] R.Rapier, "Estimating The Carbon Footprint Of Hydrogen Production," *Forbes*, June 06, 2020. Accessed Apr 20, 2023. https://www.forbes.com/sites/rrapier/2020/06/06/estimating-the-carbon-footprint-of-hydrogen-production.

[42] N.Mattsson, V.Verendel, F.Hedenus, and L.Reichenberg, "An autopilot for energy models – automatic generation of renewable supply curves, hourly capacity factors and hourly synthetic electricity demand for arbitrary world regions," *Energy Strategy Reviews*, vol. 33, January, 2021. Accessed May 02, 2023. https://www.sciencedirect.com/science/article/pii/S2211467X20301590.

[43] S.Öberg, M.Odenberger, and F.Johnsson, "The cost dynamics of hydrogen supply in future energy systems – A techno-economic study," *Applied Energy*, vol. 328, November 4, 2022. Accessed Apr 24, 2023. https://research.chalmers.se/publication/533134/file/533134-Fulltext.pdf.

[44] Energimyndigheten, "2019 rekordår för svensk elproduktion," Accessed May 15, 2023. https://www.energimyndigheten.se/nyhetsarkiv/2020/2019-rekordar-for-svensk-elproduktion/.

[45] L.Göransson, J.Goop, M.Odenberger, and F.Johnsson, "Impact of thermal plant cycling on the cost-optimal composition of a regional electricity generation system," *Applied Energy*, vol. 197, July 1, 2017. Accessed Apr 24, 2023. https://www.sciencedirect.com/science/article/pii/S0306261917304142.

[46] "EU Natural Gas," *Trading economics*. Accessed Mar 27, 2023. https://tradingeconomics.com/commodity/eu-natural-gas.

[47] "LNG import prices in selected countries, 2010-2019," *IEA*, October 26, 2022. Accessed Apr 03, 2023. https://www.iea.org/data-and-statistics/charts/lng-import-prices-in-selected-countries-2010-2019.

[48] O.Hvalbye, M.Sillasoo, and B.Schieldrop, "Natural Gas. [We expect TTF prices to move higher from here]," *SEB, Macro & FICC Research*, March 29, 2023. Accesed Apr 03, 2023. https://research.sebgroup.com/macro-ficc/reports/36989.

[49] "EU Carbon Permits," *Trading Economics*. Accessed Apr 20, 2023. https://tradingeconomics.com/commodity/carbon.

[50] B.Schieldrop, "Utility forward hedging will likely drive EUA prices rapidly higher in 2024," *SEB, Macro & FICC Research*. Accessed Apr 20, 2023. https://research.sebgroup.com/macro-ficc/reports/37565.

[51] "Electrolysers," September, 2022. Accessed Feb 01, 2023. https://www.iea.org/reports/electrolysers.

A

Figures for technologies

Table A.1: Financial figures, technical lifetimes and efficiencies for respective technology used in the reference case. Figures for the CCS are

Technology	**CAPEX,** [EUR/MW]	**Fixed O&M,** [EUR/MW/yr]	**O&M,** [EUR/MWh]	**Efficiency**	**Lifetime**
Electrolyzer	50,000[a]	24,000	0	0.65	30
SMR	-	-	110	0.80	-
Offshore wind[b]	2,115,000	90,000	1.1	-	25
LRC	11,000	-	-	-	50
LIB	135,000	0	0	0.90	15
CCS	1,900,000[c]	-	125[d]	0.90	30

[a] The investment cost for alkaline electrolyzer is retrieved from IEA's report on electrolyzers 2022 [51].
[b] Financial figures for offshore wind power is retrieved from Toktarova et al [25].
[c] Unit is EUR/tCO_2/h.
[d] Unit is EUR/tCO_2.

B

Values of necessary parameters

Table B.1: Figures for the model's parameters used in the reference case.

Parameter	Description	Value	Unit	Reference/Comment
d_t	Hydrogen demand	376.9	[MW_{H2}]	Retrieved from Preem
r_n^{smr}	Ramp rate	0.15	[-]	Retrieved from Preem
C_{smr}^{cyc}	Cycling cost	2.5	[EUR/MWh]	-
l_{smr}^{min}	Minimum load	0.50	[-]	Retrieved from Preem
γ^{smr}	Capacity SMR	297	[MW_{H2}]	Retrieved from Preem
α_{LRC}^{c}	Charge rate	0.0025	[-]	Retrieved from [22]
α_{LRC}^{d}	Discharge rate	0.005	[-]	Retrieved from [22]
$\gamma^{transmission}$	Capacity to grid	15	[MW]	Retrieved from Preem
GT	Grid tariff	90	[EUR/MWh]	-
GP	Gas price	57.4	[EUR/MWh]	Five year average
ETS	EU ETS	100	[EUR/tCO_2]	-
PPA	Power purchase agreement	56.1	[EUR/MWh]	LCOE for offshore
W	Compression work	0.0564	[MWh/MWh_{H2}]	For compression to 80 barg

C

Sensitivity analysis: Transmission capacity and forecasted spot prices

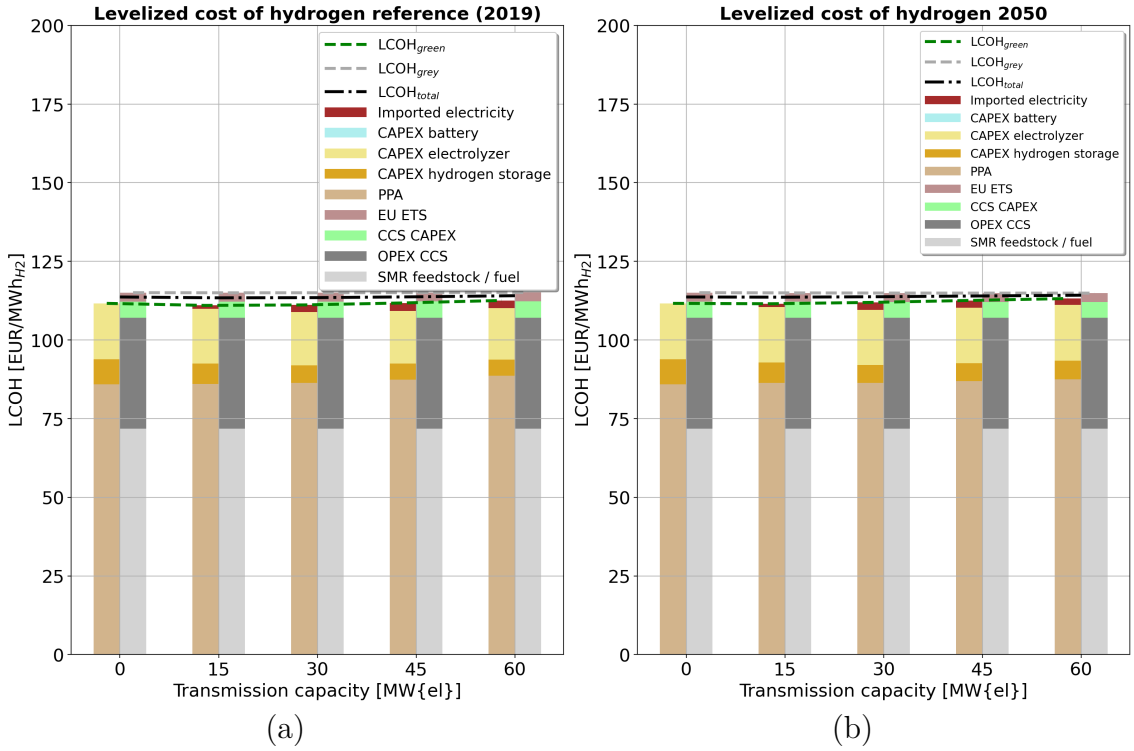

Figure C.1: Levelized cost of hydrogen for (a) 2019 and (b) 2050.

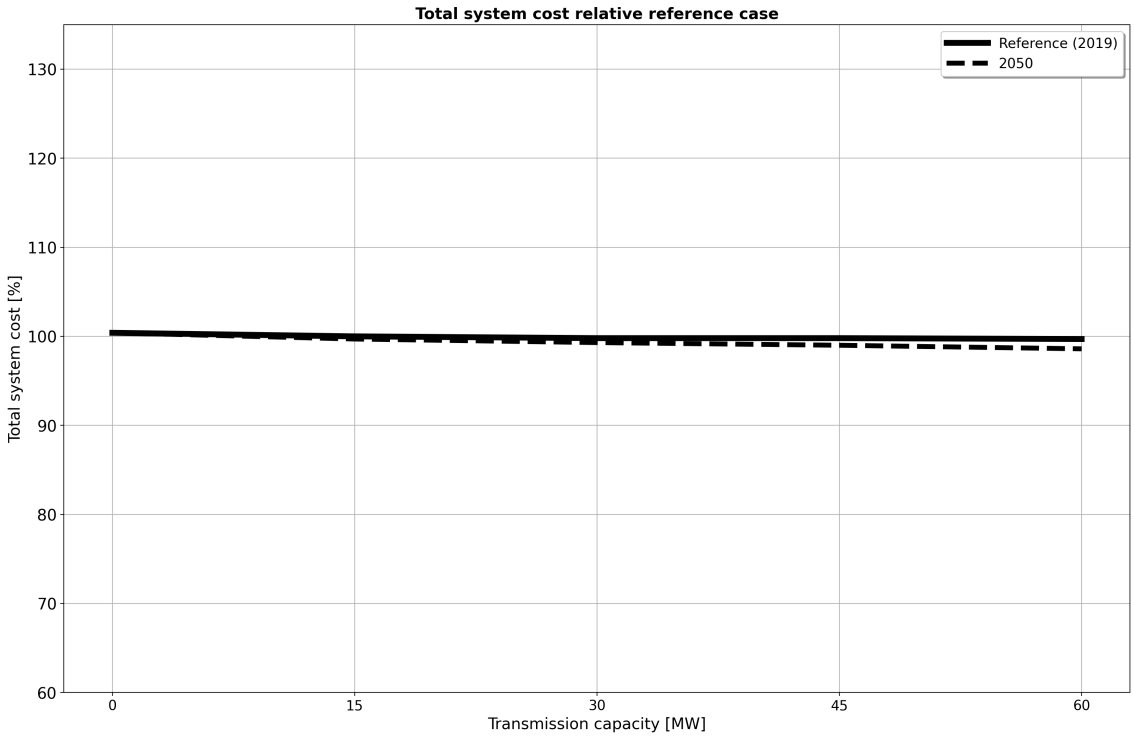

Figure C.2: The relative change in total system cost for 2019 and 2050.

DEPARTMENT OF SPACE, EARTH AND ENVIRONMENT
CHALMERS UNIVERSITY OF TECHNOLOGY
Gothenburg, Sweden
www.chalmers.se

CHALMERS
UNIVERSITY OF TECHNOLOGY